EUROPEAN RESPIRATORY journal

FLAGSHIP SCIENTIFIC JOURNAL OF ERS

Early View

Original article

# Homeostatic and Early Recruited CD101$^{-}$ Eosinophils Suppress Endotoxin-induced Acute Lung Injury

Chen Zhu, Qing-Yu Weng, Ling-Ren Zhou, Chao Cao, Fei Li, Yin-Fang Wu, Yan-Ping Wu, Miao Li, Yue Hu, Jia-Xin Shen, Xue-Fang Xiong, Fen Lan, Li-Xia Xia, Bin Zhang, Hao Zhang, Man Huang, Song-Min Ying, Hua-Hao Shen, Zhi-Hua Chen, Wen Li

Please cite this article as: Zhu C, Weng Q-Y, Zhou L-R, *et al*. Homeostatic and Early Recruited CD101$^{-}$ Eosinophils Suppress Endotoxin-induced Acute Lung Injury. *Eur Respir J* 2020; in press (https://doi.org/10.1183/13993003.02354-2019).

This manuscript has recently been accepted for publication in the *European Respiratory Journal*. It is published here in its accepted form prior to copyediting and typesetting by our production team. After these production processes are complete and the authors have approved the resulting proofs, the article will move to the latest issue of the ERJ online.

# Homeostatic and Early Recruited CD101$^{-}$ Eosinophils Suppress Endotoxin-induced Acute Lung Injury

Chen Zhu, MD, PhD,[a,#] Qing-Yu Weng, MD,[a,#] Ling-Ren Zhou, MD,[a,#] Chao Cao, MD, PhD,[b] Fei Li, MD, PhD,[a] Yin-Fang Wu, MD, PhD,[a] Yan-Ping Wu, MD, PhD,[a] Miao Li, MD, PhD,[a] Yue Hu, MD, PhD,[a] Jia-Xin Shen, MD,[a] Xue-Fang Xiong, MD,[a,c] Fen Lan, MD, PhD,[a] Li-Xia Xia, MD, PhD,[a] Bin Zhang, MD,[a] Hao Zhang, MD, PhD,[a] Man Huang, MD, PhD,[d] Song-Min Ying, MD, PhD,[a] Hua-Hao Shen, MD, PhD,[a,e,*] Zhi-Hua Chen, PhD,[a,*] Wen Li, MD, PhD,[a,*]

[a]Key Laboratory of Respiratory Disease of Zhejiang Province, Department of Respiratory and Critical Care Medicine, Second Affiliated Hospital of Zhejiang University School of Medicine, Hangzhou, Zhejiang, 310009, China;

[b]Department of Respiratory Medicine, Ningbo First Hospital, Ningbo, Zhejiang, 315000, China;

[c]Department of Respiratory Medicine, The Central Hospital of Lishui City, Lishui, Zhejiang, 323001, China;

[d]Department of Central Intensive Care Unit, Second Affiliated Hospital of Zhejiang University School of Medicine, Hangzhou, Zhejiang, 310009, China;

[e]State Key Lab for Respiratory Diseases, Guangzhou, Guangdong, 510120, China.

Authorship note:

[#]These authors contributed equally to this article.

[*]Correspondence should be addressed to W.L. (liwen@zju.edu.cn), Z.H.C. (zhihuachen@zju.edu.cn) or H.H.S. (huahaoshen@zju.edu.cn)

**Author Contributions:** C.Z., C. C., S.M.Y., Z.H.C., H.H.S. and W.L. designed and analyzed the studies. C.Z. Q.Y.W. and L.R.Z. performed the experiments. F.L. contributed to the isolation of eosinophils form NJ.1638 mice. Y.F.W.,

Y.P.W., M.L. and J.X.S. assisted with animal breeding and sacrifices of ALI and OVA models. C.C., Y.H., F.L., L.X.X., B.Z., H.Z. M.H. and X.F.X. contributed to the collection of human samples. C.Z., Z.H.C. and S.M.Y. drafted the article, and L.R.Z. with Q.Y.W. proof-read the manuscript. All the experiments were proceeded under the supervision of H.H.S., Z.H.C., and W.L. All authors approved the final manuscript.

We wish to thank Mrs. Yanwei Li and Mrs. Xinghui Song from Core facilities of Zhejiang University School of Medicine for their technical assistances in flow cytometry sorting system, Mrs. Xiaodan Wu from Analysis Center of Agrobiology and Environmental Sciences, Zhejiang University for LC/MS analysis, and all the stuff in Laboratory animal center of Zhejiang University for mice feeding. We also thank Prof. Lie Wang, Dr. Zhaoyuan Hui, and Dr. Feng Lin from Institute of Immunology, Zhejiang University School of Medicine for immunology-related advices in this study. Finally, we thank Dr. Jing Chen from Department of Oncology, Jinling Hospital, Nanjing University and Dr. Yuanjian Fang from Department of Neurosurgery, The Second Affiliated Hospital of Zhejiang University, School of Medicine for analyzing high-throughput consequences.

This work was financially supported by Major Project of NSFC (No.91642202 to W.L., No.81490532 to H.H.S.), International Cooperation Project of NSFC (No.81420108001 to H.H.S.), the National Key R&D Program of China (2016YFA0501602 to Z.H.C.), and Key Project of Chinese National Programs for Fundamental Research and Development (973 program, 2015CB553405 to Z.H.C.).

Running title: Eosinophils suppress acute lung injury

**Abstract**

**Rationale:** Acute lung injury (ALI) is a fatal but undertreated condition with severe neutrophilic inflammation, while little is known about the functions of eosinophils in pathogenesis of ALI.

**Objectives:** To investigate the roles and molecular mechanisms of eosinophils in ALI.

**Methods:** Pulmonary eosinophils were identified by flow cytometry. Mice with abundant or deficient eosinophils were used. Cellularity of eosinophils and neutrophils in BALF, inflammatory assessment, and survival rate were detected. Human samples were also used for validating experimental results.

**Results:** Blood eosinophils were increased in survived individuals of patients with acute respiratory distress syndrome independent of the corticosteroid usage. There existed homeostatic eosinophils in lung parenchyma in mice, and these homeostatic eosinophils in originating from the bone marrow were predominantly $CD101^-$. More $CD101^-$ eosinophils could be recruited earlier than lipopolysaccharide (LPS)-initiated neutrophilic inflammation. Loss of eosinophils augmented LPS-induced pulmonary injury. Homeostatic $CD101^-$ eosinophils ameliorated, while allergic $CD101^+$ eosinophils exacerbated, the neutrophilic inflammation induced by LPS. Likewise, CD101 expression in eosinophils from ARDS patients did not differ from the healthy subjects. Mechanistically, $CD101^-$ eosinophils exhibited higher levels of Alox15 and Protectin D1. Administration of Protectin D1 isomer attenuated the neutrophilic inflammation.

**Conclusions:** Collectively, our findings identify an uncovered function of native $CD101^-$ eosinophils in suppressing neutrophilic lung inflammation and suggest a potential therapeutic target for ALI.

**Keywords:** eosinophil; CD101; acute lung injury; pulmonary inflammation

## Introduction

Acute lung injury (ALI)/ acute respiratory distress syndrome (ARDS) is a clinical disorder characterized by increased pulmonary vascular permeability, massive inflammation and subsequent pulmonary edema and refractory hypoxia[1, 2], leading to a high mortality and morbidity. During the process of ALI/ARDS, accumulated inflammatory cells and cytokines induce the disruption of capillary endothelial and alveolar epithelial barrier and promote subsequent pulmonary edema and hypoxia[3]. Despite a wide variety of risk factors of ARDS[4], inhibition of pulmonary inflammation represents a common therapeutic strategy for this critical syndrome.

Eosinophils are known as the terminal effector cells during parasite infection or allergic inflammation, but growing evidence has demonstrated their regulatory effects in various immune responses[5]. It has been reported that eosinophils interact with DCs to synergistically promote the Th2 immune response in the allergic airway[6, 7]. Interestingly, a recent clinical investigation showed that the ALI survivors exhibited an increased number of eosinophils in the lung compared to the non-survivors[8], suggesting a protective role of eosinophils in ALI. Conversely, patients with eosinophil dominant diseases, such as asthma, appear to be at high risks for infection[9]. Hence, the eventual functions of eosinophils and their molecular mechanisms in the pathogenesis of ALI require further investigations.

Tissue resident cells frequently demonstrate unique functions in maintaining the milieu of certain organ or system. Lung resident AMs are known to display distinctive origin, surface markers, and functions[10, 11]. While resident eosinophil subgroup was mostly identified in tissues like gastrointestinal tract, adipose tissue, uterus, spleen, thymus, or mammary glands[12], Mesnil *et al.* have recently demonstrated that there are also homeostatic eosinophils in the lung[13]. This study also implies that the SiglecF$^{+}$CD125$^{+}$ eosinophils display distinctive subgroups distinguished by CD101. Nonetheless, little is known about the origination and the functions of lung homeostatic eosinophils,

especially in non-eosinophilic diseases.

The present study aims to explore the origination and function of lung eosinophils in an endotoxin-induced ALI model using eosinophil-deficient PHIL mice. We also provide evidence that homeostatic $CD101^-$ and allergy-induced $CD101^+$ eosinophils exert distinct functions in ALI through different molecular mechanisms.

## Methods

Additional details on methods are available in online supplements.

*Statistics analysis.* The statistical graphs of each experiment were illustrated by GraphPad 7.0 software, and data were shown as means ± SD. For statistics analysis, two-tailed Students *t* test and One-way ANOVA were used unless otherwise specified. For surviving curve analysis, Mantel Cox test was used. Categorical variables in patients' information were analyzed by Pearson's chi square tests. A significance was accepted at $p$ value <0.05.

## Results

### Increased blood eosinophil cellularity in survived ARDS patients is independent of corticosteroid usage

We first examined the clinical relevance of eosinophils in ALI. It is ethically not correct to undertake lung biopsy of the ALI/ARDS patients due to the potential risks. Thus, we performed a retrospective analysis referring to all the ARDS diagnosed inpatients of our hospital from 2012 to date. The brief demographic profiles were summarized in Table S1 and the inclusion criteria was presented in Fig. 1A. We did not observe any difference in the amount of blood eosinophils amongst healthy controls, survived ARDS patients, and non-survived ARDS patients at basal levels. Interestingly, the survived individuals displayed an elevated eosinophil cellularity following clinical treatment, whereas the non-survivors did not. (Fig. 1B). We further analyzed

the doses of corticosteroid used in these patients and found that there were insignificant differences in the levels of corticosteroid usage, either intravenously (systemically) or inhaled, between survivors and non-survivors of ARDS patients (Fig. 1C and D). These data suggest that increased levels of blood eosinophils are associated with an increased survival in ARDS patients, independent of the usage of corticosteroid.

**Homeostatic and early induced eosinophils during ALI are localized in lung parenchyma**

To assess the possible function of eosinophils in the pathogenesis of ALI, we examined the homeostasis and flux of lung eosinophils in Lipopolysaccharide (LPS)-induced ALI. In our study, eosinophils were identified as $CD45^+SiglecF^+F4/80^+CD11b^+CD11c^-$, AMs were labeled as $CD45^+SiglecF^+F4/80^+CD11b^-CD11c^+$ according to previous reports[10, 14], and neutrophils were defined as $CD45^+Gr\text{-}1^{hi}CD11b^{hi}$ (Fig. 2A). The gate strategy was simplified for the assays where neutrophils were not stained[15] (Fig. S1). In agreement with previous findings[13], there existed a notable amount of “resident” eosinophils at basal condition in the lung (Fig. 2B). Interestingly, the number of pulmonary eosinophils was comparable with AMs and was much higher than that in circulation (Fig. S2). More intriguingly, a rapid but transient increase of eosinophils was observed within 30 mins after LPS exposure, while neutrophils were elevated remarkably later after 2h (Fig. 2B). Similarly, the total inflammatory cells and the number of neutrophils in bronchoalveolar lavage fluid (BALF) were also significantly increased after 2 h (Fig. 2C and Fig. S3). Also, the early induction of pulmonary eosinophils was validated by *S. aureus* injection *i.t.* in mice (Fig. S4).

Surprisingly, eosinophils were not detectable in BALF (Fig. 2C). The Congo red staining (Fig.2D) and EPX immunohistochemistry staining (Fig.2E) suggested that lung “resident” eosinophils were located in lung parenchyma. To obtain a better visible evidence, CD45.1 wildtype mice were intravenously

injected with CD45.2 eosinophils (from NJ.1638 mice) at $1x10^6$, and right after the injection, the lung sections were collected for immunofluorescence staining of CD45.2. The results revealed that intravenous flushing eliminated majority of circulating cells (Fig. S5), and there was still $CD45.2^+$ eosinophils in perivascular area or lung parenchyma (Fig. 2F). These results suggest that circulating eosinophils readily migrate to and reside in lung parenchyma during homeostasis, and could be further recruited during the initiation of ALI.

**Lung parenchymal eosinophils are originated from bone marrow and are recruited from peripheral blood**

Previous study have classified pulmonary eosinophils as “resident” or “inflammatory”[13]. To explore the origin of “resident” and LPS-induced parenchymal eosinophils, we established several chimera mice. Firstly, WT or PHIL mice received total bone marrow transplant from WT or PHIL mice by tail vein injection following irradiation (Fig. 3A). PHIL mice are eosinophil deficiency due to insertion of diphtheria toxin A (DTA) in eosinophil peroxidase (EPX) promoter (Fig. S6). At 1 month after bone marrow reconstitution, eosinophils were uniquely diminished in lung tissue of PHIL→WT mice but were repopulated in that of WT→PHIL mice (Fig. 3A). To further verify this phenotype, CD45.2 WT mice were used as recipients, whereas CD45.1 WT mice were used as donors (Fig. 3B). Within 1 month of bone marrow transfer, in those CD45.1→CD45.2 chimera mice, the pulmonary eosinophils were repopulated as CD45.1 in a time-dependent manner (Fig. 3B), while lung resident macrophages (AMs) remained predominantly as CD45.2 (Fig. S7).

To further clarify whether eosinophils could be recruited during ALI, $5x10^5$ eosinophils were injected to PHIL mice through tail vein, and the mice were immediately challenged with LPS (Fig. 3D). Intriguingly, after LPS administration, eosinophils were notably accumulated in lung tissue, and there was a synchronous decrease of eosinophils in peripheral blood (Fig. 3D). We also validated the rapid recruitment of eosinophils in WT mice. CD45.1 mice

were received CD45.2 eosinophils via tail vein and were subsequently challenged with LPS (Fig. 3E). Similarly, the amount of CD45.2 eosinophils was significantly increased in the lung after LPS instillation (Fig. 3E, FACS and scatter images). Interestingly, the induction of eotaxin was later (2 hours) than the increase of eosinophils (30 mins) after LPS challenge (Fig. S8), suggesting that LPS-induced early recruitment of eosinophils might be eotaxin-independent.

Several additional experiments were conducted to test whether lung "resident" eosinophils could undergo local replication upon LPS treatment. *In vivo*, WT mice were received BrdU injection. Similarly, pulmonary eosinophils displayed BrdU negative, while circulating monocyte ($CD45^+CD115^+$) exhibited $BrdU^+$ subsets (Fig. S9A). Again, very few sorted eosinophils displayed as an EdU positive cluster, whereas as a positive control, eosinophil cell line Eol-1 was stained isochronously. (Fig. S9B). Finally, when colony forming assay was performed, we did not observe any colony in sorted eosinophil group. (Fig. S9C).

Taken together, these data demonstrate that the "resident" parenchymal eosinophils originate from bone marrow, and recruitment of pulmonary eosinophils from peripheral blood occurs during homeostasis or rapidly upon pathogen exposure.

**Eosinophil deficiency exacerbates LPS-initiated pulmonary inflammation and ALI**

To investigate the role of eosinophils during the initiation of ALI, PHIL mice were challenged with LPS. As shown in Fig.4A, the neutrophilic inflammation in lung tissue of PHIL mice was evidenced earlier than that of WT mice. Additionally, the inflammatory cells and cytokines in BALF (Fig. 4B and C) were significantly increased in PHIL mice during the initiation of ALI.

To assess the eventual levels of ALI, the inflammatory hallmarks were examined 24 hours after LPS administration. Consistently, inflammation in

LPS-treated PHIL mice was augmented compared to WT mice, as evidenced by leukocyte infiltration (Fig. S10A), and inflammatory mediators in BALF (Fig. S10B). Similarly, PHIL mice also displayed an exacerbation of pulmonary inflammation when exposed to *S. aureus* (Fig. S11). Consistent with these findings, pulmonary edema (Fig.4D), endothelial leakage (Fig. 4E and F) and elastance (Fig. 4G) were also more severe in LPS-treated PHIL mice. Consequently, we observed a decrease in both body weight (Fig. S10C) and assessment score (Fig. S10D) of PHIL mice. Furthermore, PHIL mice still displayed elevated levels of pulmonary inflammation 72 hours after LPS instillation (Fig. 4H) and eventually experienced higher mortality as compared to LPS challenged WT mice (Fig. 4I).

Thus, eosinophil deficiency leads to enhanced inflammation and consequent poorer living status. All the above described results indicate that the lung “resident” and the early induced eosinophils might be crucial characters in inhibiting the initiation of ALI.

**CD101 is a marker to distinguish different subtypes of eosinophils**

The above results suggest a protective role of eosinophils in ALI, which seems not allied with the clinical evidence that allergic patients are susceptible to infection[9, 16, 17]. Thus, we established an OVA/LPS model as schemed in Fig. 5A. Interestingly, we observed that earlier OVA challenge notably exacerbated the LPS-induced infiltration of leukocyte in BALF (Fig. 5B), regardless of the higher levels of eosinophils in the lung induced by OVA (Fig. S12).

To explore the paradoxical effects of eosinophils in the process of ALI pathogenesis, we analyzed the heterogeneity of eosinophils and observed two subgroups, $CD101^-$ and $CD101^+$ of eosinophils in lung tissues. Under normal conditions, $CD101^-$ eosinophils were the majority; however, in OVA-challenged lung tissue, the levels of $CD101^+$ eosinophils were higher than that of $CD101^-$ (Fig. 5C).

Similarly, the major subgroup of eosinophils in peripheral blood and bone marrow was again $CD101^-$ predominant at steady stage (Fig. 5D). OVA challenge significantly induced both $CD101^-$ and $CD101^+$ eosinophils in bone marrow and blood, however, the majority was still $CD101^-$ (Fig. 5D). LPS treatment at early times failed to alter the CD101 levels of eosinophils in periphery (Fig. S13). Additionally, we also conducted the bone marrow derived eosinophil differentiation *in vitro* and observed that the differentiated eosinophils induced by interleukin-5 (IL-5) were predominantly $CD101^-$ (Fig. 5E). Likewise, eosinophils from peripheral blood of IL-5-transgenic NJ.1638 mice were also predominantly $CD101^-$, and the factors involved in eosinophil differentiation, or house dust mite extraction (HDM), could not induce the $CD101^-$ eosinophils to be positive (Fig. S14).

To further explore the relevance of our results in human, we also detected the expression of CD101 in eosinophils from both non-asthmatics and asthmatic patients. Not surprisingly, the asthmatic patients displayed higher eosinophil cellularity in peripheral blood (Fig. 5F). Likewise, the expression of CD101 was significantly elevated in eosinophils from asthmatic patients (Fig. 5G).

Taken together, these data suggest that CD101 is a marker to distinguish eosinophils between their naive and allergy-induced status, and that molecules other than IL-5 and GM-CSF might drive $CD101^-$ eosinophils to be positive in allergic microenvironment.

**$CD101^-$ eosinophils ameliorated, while $CD101^+$ eosinophils exacerbated, the neutrophilic inflammation induced by LPS**

We next examined the possible different functions of the subtypes of eosinophils during the process of initiation of ALI. Interestingly, most of the increased eosinophils upon LPS challenge in the lungs were $CD101^-$ (Fig.6A), and similarly, the amount of $CD101^-$ eosinophils showed isochronous aggregation in *S. aureus* infection (Fig. S15), suggesting that the $CD101^-$ and

$CD101^+$ eosinophils may play distinct roles in ALI pathogenesis. To address this, $CD101^-$ or $CD101^+$ eosinophils were isolated from OVA-induced allergic mice, and were adoptively transferred into PHIL mice, followed with LPS challenge. The efficacy of adoptive transfer is presented as Fig. S16. Intriguingly, $CD101^-$ eosinophils relieved while $CD101^+$ eosinophils exacerbated LPS-induced early leukocyte aggregation (Fig. 6B) and cytokine production (Fig.6C). Similar effects were observed in these mice 24 h after LPS challenge. Following adoptive transfer, $CD101^-$ eosinophils decreased, yet $CD101^+$ eosinophils augmented, the eventual inflammation, as evidenced by leukocyte amounts (Fig. 6D), expression of certain cytokines and chemokines (Fig. 6E), and pathological scores (Fig. 6F). Unlike the high expression of CD101 in eosinophils from asthmatic patients (as a positive control), the levels of CD101 in eosinophils from ARDS patients were much lower and comparable to the health subjects (Fig. 6G). To test whether these two subsets of eosinophils exhibited differential expression of the critical signaling in response to LPS challenge, we detected the levels of toll-like receptor 4 (TLR4)-related molecules and inflammatory cytokines in each subset of eosinophils, and found that there was no difference in these eosinophils between both control and LPS treated groups (Fig. S17).

Moreover, we examined the effects of eosinophils in both “prevention” and “resolution” models. The prevention model was schemed as (Fig. S18A). As predicted, transferred $CD101^-$ eosinophils prevented ALI inflammation, whereas $CD101^+$ eosinophils exacerbated LPS-induced inflammation (Fig. S18B and C). The resolution model was schemed as (Fig. S16D). To our surprise, transferred $CD101^-$ eosinophils after LPS injection only showed transitory protection (Fig. S18E and F).

Nonetheless, these data altogether demonstrate that $CD101^-$ eosinophils exhibit an anti-inflammatory effect and eventually attenuate, while $CD101^+$ eosinophils further promote, the neutrophilic inflammation and ALI.

**Alox15 and Protectin D1 are associated with the anti-inflammatory effect of CD101$^-$ eosinophils in ALI**

Since CD101$^-$ and CD101$^+$ eosinophils exerted distinct effects on inflammation, we next explored the possible dissimilarities of these subtypes of cells via RNA sequencing. By comparing the transcriptomes between CD101$^-$ and CD101$^+$ eosinophils, we noticed that Alox15 was more abundant in the CD101$^-$ eosinophils (Fig. 7A) and this result was confirmed by quantitive PCR (Fig. 7B). Interestingly, the expression of Alox15 was tightly associated with emerged eosinophils in ALI. In lung homogenates, Alox15 was also increased in 30 mins after LPS instillation (Fig. 7C), and LPS failed to induce Alox15 expression in PHIL mice (Fig. 7D). By comparing the Alox15 expression in eosinophils from NJ. 1638 mice (CD101$^-$) with that of lung homogenates, we illustrated that CD101$^-$ eosinophils expressed much higher levels of Alox15 than other pulmonary cells (Fig. 7E).

Alox15 (also referred as 12/15-LO in mice or 15-LOX in human) is the key enzyme known to convert docosahexaenoic acid (DHA) into anti-inflammatory lipid mediators like Protectin D1 (10R, 17S- dihydroxy-docosa-4Z, 7Z, 11E, 13E, 15Z, 19Z-hexaenoic acid)[18, 19], hence we reasoned that CD101$^-$ eosinophils might attenuate the initiation of inflammation of ALI by influencing the lipidomic profiles in lung. LC/MS-based lipid analysis was performed with CD101$^-$ and CD101$^+$ eosinophils, as well as lung tissues from both PHIL and WT mice to detect Protectin D1 abundance (Fig. 7F-H). As predicted, Protectin D1 was more abundant in CD101$^-$ eosinophils compared to CD101$^+$ eosinophils, and WT lung homogenates had more Protectin D1 than PHIL mice. The results above were congruent with Alox15 expression in mRNA level, suggesting that CD101$^-$ eosinophils might influence inflammation initiation through Alox15-mediated production of Protectin D1.

Treatment of PD1-isomer (PDx) is known to mimic the effect of Protectin D1 administration[20]. As expected, intraperitoneal injection of PDx ameliorated the onset of LPS-induced inflammation in PHIL mice (Fig. 7I). Furthermore,

Alox15 inhibitor PD146176 administration exacerbated initiative neutrophil accumulation in WT-LPS mice (Fig. 7J).

For further validation, we also detected the expression of ALOX15 and Protectin D1 in human eosinophils of both asthmatic and non-asthmatic individuals. Congruent with the results in mice, eosinophils of the non-allergic subjects displayed elevated expression of ALOX15 (Fig. 7K) and increased secretion of Protectin D1 (Fig.7L) compared to asthmatic eosinophils.

These findings further substantiate that Alox15-mediated Protectin D1 from $CD101^-$ eosinophils is a predominant signature that attenuates neutrophil infiltration in the initiation of endotoxin-induced ALI.

## Discussion

In our study, we demonstrate that the “resident” eosinophils in lung parenchyma, are predominantly $CD101^-$, which are derived from bone marrow. LPS challenge causes a rapid accumulation of eosinophils into lungs from peripheral circulation. Loss of eosinophils augments the LPS-induced neutrophilic inflammation and the eventual levels of ALI. Homeostatic $CD101^-$, but not allergic $CD101^+$, eosinophils exert anti-inflammatory function in ALI, likely via the Alox15-mediated production of Protectin D1 (Fig. 8).

Eosinophil accumulation in non-allergic diseases is easily overlooked, and in fact eosinophils have been involved in tumorigenesis[21], bowel inflammatory diseases[20, 22],and hematopoietic stem cell homeostasis[23]. In ALI patients, the survivors displayed an increased in the number of eosinophils in lung compared to the non-survivors[8]. We also observed increased levels of eosinophils in peripheral blood of survival ARDS patients, which suggest that eosinophils may exert a protective effect on ALI. Our current study provides more experimental evidence and mechanistic details involving how homeostatic and early-recruited $CD101^-$ eosinophils exhibit an anti-inflammatory character in endotoxin-induced ALI.

Mechanistically, the protective effect of $CD101^-$ eosinophils might be

associated with the Alox15-mediated production of Protectin D1. Lipid synthetization is involved in granulocyte development[24], recruitment[25], and other inflammation. In inflamed tissues, synthesized Protectin D1 could block neutrophil recruitment [20], and simultaneously stimulates non-inflamed removal of neutrophils debris[26]. It has been shown that eosinophils express higher level of Alox15 compared to neutrophils[27], which suggest that eosinophils might be the main originating cells involved in the biosynthesis of Protectin D1. Furthermore, Protectin D1 is down-regulated in both asthmatic patients and mice [18, 27], which corroborates our findings in the asthmatic and non-asthmatic eosinophils in human, and also $CD101^+$ eosinophils and $CD101^-$ eosinophils in mice. Exogenous administration of either Protectin D1 or its isomer PDx attenuates recruitment of inflammatory cell [20, 26, 28] and decreases inflammatory cytokines expression[28], thereby limits inflammatory process, which is consistent with our current observations.

Intriguingly, as the data shown in “prevention” and “resolution” models (Fig. S16), the efficacy of $CD101^-$ eosinophils in limiting LPS-induced pulmonary inflammation in prevention model was superior to that in resolution model. The detailed mechanisms for such a difference were not clear. We hypothesized that $CD101^-$ eosinophils might take effect only after they “are located in their position” in lung parenchyma during homeostasis; however large amounts of neutrophils destroyed the functional microenvironment of $CD101^-$ eosinophils after inflammation outburst.

On the contrary, adoptive transfer of $CD101^+$ eosinophils deteriorated LPS-induced ALI. $CD101^+$ eosinophils are mainly enhanced in asthmatic inflammation, highly implying that asthmatic patients might not benefit from eosinophil infiltration in lung injury [9]. Based on the results from RNAseq, it is plausible to hypothesize that the pro-inflammatory function of $CD101^+$ eosinophils is due to the overexpression of alarmins, like S100a8 and S100a9 (Fig. 7A), since these alarmins have been shown to enhance the development and influx of monocyte and neutrophils [25, 29].

$CD101^+$ eosinophils are noticed in asthmatic mice accompanied with a few $CD101^-$ eosinophils. However, in asthmatic patients, eosinophils display $CD101^{hi}$ eosinophils only. This discrepancy is likely due to either the diversity in duration of asthma or the difference between human eosinophils and murine eosinophils. Furthermore, $CD101^+$ eosinophils accompanies frequently with CD62L shedding[13]. However, we observed that the expression of CD62L was very low in pulmonary eosinophils, irrespective of being either $CD101^-$ or $CD101^+$, or homeostatic or allergy-induced (data not shown). Therefore, we used CD101, but not CD62L, as a marker to distinguish the different eosinophil subgroups in this study.

In both asthma and endotoxin-induced ALI, the transformation of $CD101^-$ to $CD101^+$ in eosinophils is of great significance. We observed that the expression of CD101 in eosinophils is independent of the process of eosinophil development-related cytokines or HDM exposure (Fig. S13). A recent study demonstrates a crucial role of IL-18 in the transformation of eosinophils[30], however, the molecular spectrum which promotes the transformation of eosinophils is still unclear.

Tissue resident immune cells are known to have prominent effects in maintaining homeostasis of a certain milieu[31]. In our study, we demonstrated that the lung was an important organ for eosinophil residence, and also observed that parenchymal eosinophil population was bone-marrow-dependent. These data strongly suggest that lung eosinophils are rather “homeostatic” than “resident”. Although, we demonstrate a recruitment of eosinophils during ALI initiation, the mechanisms mediating the recruitment are not clear. At the early time points after LPS challenge, we failed to observe any induction of eotaxins before eosinophil aggregation. Previously, it has been reported that LPS induces eosinophil migration in pleurisy independent of eotaxin[32]. Likewise, the amount of pulmonary eosinophils at steady stage remained intact in $CCR3^{-/-}$ mice[32]. Considering the high expression of the integrin family, such as Igtax and Igtae, in

eosinophils[33], it is plausible to hypothesize that eosinophils migrate to lung tissues during homeostasis or upon pathogen exposure via an eotaxin-CCR3 independent axis, which needs to be clarified in future studies.

It is of great interests to note that circulating eosinophils are increased in survived ARDS patients, suggesting that the levels of peripheral eosinophils could indeed serve as a new biomarker and a target of ALI therapy. Augmented eosinophils could display anti-pathogen activity in host defense by releasing their cationic proteins[34] and even extracellular traps[35]. Besides, eosinophils also accumulate and participate in prompting the process of tissue repair after damage[12]. Clinically, therapy with anti-IL-5 monoclonal antibody, such as mepolizumab, is wildly used for both asthmatic[36] and eosinophilic COPD patients[37], resulting in a reduced eosinophil levels in peripheral blood[36-38]. Although there is a lack of experimental evidence, it is likely that anti-IL-5 antibody would reduce both eosinophils subgroups. Theoretically, the reduction of $CD101^+$ eosinophils will benefit both asthma and ALI patients; however, the reduction of homeostatic $CD101^-$ eosinophils might increase the risks and levels of ALI. Thus, our study suggests that the scheme of anti-IL-5 therapy for eosinophilic airway inflammation should be neatly controlled to reduce the risks for infection.

In summary, our findings uncover a function of homeostatic and rapidly recruited $CD101^-$ eosinophils in lung parenchyma for the suppression of endotoxin-induced ALI via the Alox15-Protectin D1 axis, and suggest a new biomarker and a potential therapeutic target for ALI.

## Conflict of Interest

All the authors have cautiously inspected the manuscript and declare no conflict of interest.

## References

1. Fan E, Del Sorbo L, Goligher EC, Hodgson CL, Munshi L, Walkey AJ,

Adhikari NKJ, Amato MBP, Branson R, Brower RG, Ferguson ND, Gajic O, Gattinoni L, Hess D, Mancebo J, Meade MO, McAuley DF, Pesenti A, Ranieri VM, Rubenfeld GD, Rubin E, Seckel M, Slutsky AS, Talmor D, Thompson BT, Wunsch H, Uleryk E, Brozek J, Brochard LJ, American Thoracic Society ESoICM, Society of Critical Care M. An Official American Thoracic Society/European Society of Intensive Care Medicine/Society of Critical Care Medicine Clinical Practice Guideline: Mechanical Ventilation in Adult Patients with Acute Respiratory Distress Syndrome. *Am J Respir Crit Care Med* 2017: 195(9): 1253-1263.

2. Butt Y, Kurdowska A, Allen TC. Acute Lung Injury: A Clinical and Molecular Review. *Arch Pathol Lab Med* 2016: 140(4): 345-350.

3. Bellani G, Laffey JG, Pham T, Fan E, Brochard L, Esteban A, Gattinoni L, van Haren F, Larsson A, McAuley DF, Ranieri M, Rubenfeld G, Thompson BT, Wrigge H, Slutsky AS, Pesenti A, Investigators LS, Group ET. Epidemiology, Patterns of Care, and Mortality for Patients With Acute Respiratory Distress Syndrome in Intensive Care Units in 50 Countries. *JAMA* 2016: 315(8): 788-800.

4. Ward PA, Fattahi F, Bosmann M. New Insights into Molecular Mechanisms of Immune Complex-Induced Injury in Lung. *Front Immunol* 2016: 7: 86.

5. Rosenberg HF, Dyer KD, Foster PS. Eosinophils: changing perspectives in health and disease. *Nature reviews Immunology* 2013: 13(1): 9-22.

6. Jacobsen EA, Ochkur SI, Pero RS, Taranova AG, Protheroe CA, Colbert DC, Lee NA, Lee JJ. Allergic pulmonary inflammation in mice is dependent on eosinophil-induced recruitment of effector T cells. *The Journal of experimental medicine* 2008: 205(3): 699-710.

7. Jacobsen EA, Zellner KR, Colbert D, Lee NA, Lee JJ. Eosinophils regulate dendritic cells and Th2 pulmonary immune responses following allergen provocation. *Journal of immunology* 2011: 187(11): 6059-6068.

8. Willetts L, Parker K, Wesselius LJ, Protheroe CA, Jaben E, Graziano P, Moqbel R, Leslie KO, Lee NA, Lee JJ. Immunodetection of occult eosinophils

in lung tissue biopsies may help predict survival in acute lung injury. *Respiratory research* 2011: 12: 116.

9. Juhn YJ. Risks for infection in patients with asthma (or other atopic conditions): is asthma more than a chronic airway disease? *The Journal of allergy and clinical immunology* 2014: 134(2): 247-257; quiz 258-249.

10. Hussell T, Bell TJ. Alveolar macrophages: plasticity in a tissue-specific context. *Nature reviews Immunology* 2014: 14(2): 81-93.

11. Ginhoux F, Guilliams M. Tissue-Resident Macrophage Ontogeny and Homeostasis. *Immunity* 2016: 44(3): 439-449.

12. Weller PF, Spencer LA. Functions of tissue-resident eosinophils. *Nat Rev Immunol* 2017: 17(12): 746-760.

13. Mesnil C, Raulier S, Paulissen G, Xiao X, Birrell MA, Pirottin D, Janss T, Starkl P, Ramery E, Henket M, Schleich FN, Radermecker M, Thielemans K, Gillet L, Thiry M, Belvisi MG, Louis R, Desmet C, Marichal T, Bureau F. Lung-resident eosinophils represent a distinct regulatory eosinophil subset. *J Clin Invest* 2016: 126(9): 3279-3295.

14. Sinclair C, Bommakanti G, Gardinassi L, Loebbermann J, Johnson MJ, Hakimpour P, Hagan T, Benitez L, Todor A, Machiah D, Oriss T, Ray A, Bosinger S, Ravindran R, Li S, Pulendran B. mTOR regulates metabolic adaptation of APCs in the lung and controls the outcome of allergic inflammation. *Science* 2017: 357(6355): 1014-1021.

15. Stevens WW, Kim TS, Pujanauski LM, Hao X, Braciale TJ. Detection and quantitation of eosinophils in the murine respiratory tract by flow cytometry. *Journal of immunological methods* 2007: 327(1-2): 63-74.

16. Juhn YJ, Kita H, Yawn BP, Boyce TG, Yoo KH, McGree ME, Weaver AL, Wollan P, Jacobson RM. Increased risk of serious pneumococcal disease in patients with asthma. *The Journal of allergy and clinical immunology* 2008: 122(4): 719-723.

17. Patella V, Bocchino M, Steinhilber G. Asthma is associated with increased susceptibility to infection. *Minerva medica* 2015: 106(4 Suppl 3): 1-7.

18. Levy BD, Kohli P, Gotlinger K, Haworth O, Hong S, Kazani S, Israel E, Haley KJ, Serhan CN. Protectin D1 is generated in asthma and dampens airway inflammation and hyperresponsiveness. *Journal of immunology* 2007: 178(1): 496-502.

19. Serhan CN, Chiang N, Van Dyke TE. Resolving inflammation: dual anti-inflammatory and pro-resolution lipid mediators. *Nature reviews Immunology* 2008: 8(5): 349-361.

20. Masterson JC, McNamee EN, Fillon SA, Hosford L, Harris R, Fernando SD, Jedlicka P, Iwamoto R, Jacobsen E, Protheroe C, Eltzschig HK, Colgan SP, Arita M, Lee JJ, Furuta GT. Eosinophil-mediated signalling attenuates inflammatory responses in experimental colitis. *Gut* 2015: 64(8): 1236-1247.

21. De Palma M, Biziato D, Petrova TV. Microenvironmental regulation of tumour angiogenesis. *Nature reviews Cancer* 2017: 17(8): 457-474.

22. Griseri T, Arnold IC, Pearson C, Krausgruber T, Schiering C, Franchini F, Schulthess J, McKenzie BS, Crocker PR, Powrie F. Granulocyte Macrophage Colony-Stimulating Factor-Activated Eosinophils Promote Interleukin-23 Driven Chronic Colitis. *Immunity* 2015: 43(1): 187-199.

23. Zhang C, Yi W, Li F, Du X, Wang H, Wu P, Peng C, Luo M, Hua W, Wong CC, Lee JJ, Li W, Chen Z, Ying S, Ju Z, Shen H. Eosinophil-derived CCL-6 impairs hematopoietic stem cell homeostasis. *Cell research* 2018: 28(3): 323-335.

24. Riffelmacher T, Clarke A, Richter FC, Stranks A, Pandey S, Danielli S, Hublitz P, Yu Z, Johnson E, Schwerd T, McCullagh J, Uhlig H, Jacobsen SEW, Simon AK. Autophagy-Dependent Generation of Free Fatty Acids Is Critical for Normal Neutrophil Differentiation. *Immunity* 2017: 47(3): 466-480 e465.

25. Soehnlein O, Steffens S, Hidalgo A, Weber C. Neutrophils as protagonists and targets in chronic inflammation. *Nature reviews Immunology* 2017: 17(4): 248-261.

26. Schwab JM, Chiang N, Arita M, Serhan CN. Resolvin E1 and protectin D1 activate inflammation-resolution programmes. *Nature* 2007: 447(7146):

869-874.

27. Miyata J, Fukunaga K, Iwamoto R, Isobe Y, Niimi K, Takamiya R, Takihara T, Tomomatsu K, Suzuki Y, Oguma T, Sayama K, Arai H, Betsuyaku T, Arita M, Asano K. Dysregulated synthesis of protectin D1 in eosinophils from patients with severe asthma. *The Journal of allergy and clinical immunology* 2013: 131(2): 353-360 e351-352.

28. Arita M, Bianchini F, Aliberti J, Sher A, Chiang N, Hong S, Yang R, Petasis NA, Serhan CN. Stereochemical assignment, antiinflammatory properties, and receptor for the omega-3 lipid mediator resolvin E1. *The Journal of experimental medicine* 2005: 201(5): 713-722.

29. Vogl T, Eisenblatter M, Voller T, Zenker S, Hermann S, van Lent P, Faust A, Geyer C, Petersen B, Roebrock K, Schafers M, Bremer C, Roth J. Alarmin S100A8/S100A9 as a biomarker for molecular imaging of local inflammatory activity. *Nature communications* 2014: 5: 4593.

30. Venkateshaiah SU, Mishra A, Manohar M, Verma AK, Rajavelu P, Niranjan R, Wild LG, Parada NA, Blecker U, Lasky JA, Mishra A. A critical role for IL-18 in transformation and maturation of naive eosinophils to pathogenic eosinophils. *The Journal of allergy and clinical immunology* 2018.

31. Soehnlein O, Lindbom L. Phagocyte partnership during the onset and resolution of inflammation. *Nature reviews Immunology* 2010: 10(6): 427-439.

32. Penido C, Castro-Faria-Neto HC, Vieira-de-Abreu A, Figueiredo RT, Pelled A, Martins MA, Jose PJ, Williams TJ, Bozza PT. LPS induces eosinophil migration via CCR3 signaling through a mechanism independent of RANTES and Eotaxin. *American journal of respiratory cell and molecular biology* 2001: 25(6): 707-716.

33. Wu D, Molofsky AB, Liang HE, Ricardo-Gonzalez RR, Jouihan HA, Bando JK, Chawla A, Locksley RM. Eosinophils sustain adipose alternatively activated macrophages associated with glucose homeostasis. *Science* 2011: 332(6026): 243-247.

34. Ravin KA, Loy M. The Eosinophil in Infection. *Clinical reviews in allergy &*

*immunology* 2016: 50(2): 214-227.

35. Yousefi S, Gold JA, Andina N, Lee JJ, Kelly AM, Kozlowski E, Schmid I, Straumann A, Reichenbach J, Gleich GJ, Simon HU. Catapult-like release of mitochondrial DNA by eosinophils contributes to antibacterial defense. *Nature medicine* 2008: 14(9): 949-953.

36. Ortega HG, Liu MC, Pavord ID, Brusselle GG, FitzGerald JM, Chetta A, Humbert M, Katz LE, Keene ON, Yancey SW, Chanez P, Investigators M. Mepolizumab treatment in patients with severe eosinophilic asthma. *The New England journal of medicine* 2014: 371(13): 1198-1207.

37. Pavord ID, Chanez P, Criner GJ, Kerstjens HAM, Korn S, Lugogo N, Martinot JB, Sagara H, Albers FC, Bradford ES, Harris SS, Mayer B, Rubin DB, Yancey SW, Sciurba FC. Mepolizumab for Eosinophilic Chronic Obstructive Pulmonary Disease. *The New England journal of medicine* 2017: 377(17): 1613-1629.

38. Pavord ID, Korn S, Howarth P, Bleecker ER, Buhl R, Keene ON, Ortega H, Chanez P. Mepolizumab for severe eosinophilic asthma (DREAM): a multicentre, double-blind, placebo-controlled trial. *Lancet* 2012: 380(9842): 651-659.

**Figure Legends**

**Fig. 1 Retrospective analysis of eosinophil cellularity and prognosis in ARDS inpatients.** A total of 118 ARDS inpatients were filtered, and the remained cases were divided into survivors and non-survivors groups for further analysis. **(A)** Including criteria of the analysis. **(B)** Blood eosinophil cellularity in healthy volunteers, survived and non-survived ARDS patients. HC, healthy control; ADM, 24h within hospitalization; DIS, no more than 24h before discharged or declaration of death. **(C and D)** Corticosteroid administration in ARDS patients. **(C)** Daily dose of intravenous use of corticosteroid. **(D)** Daily dose of inhaled corticosteroid. ns, no significance, **P<0.01, ***P<0.001.

**Fig. 2 Analysis of homeostatic and early induced eosinophils in lung parenchyma. (A)** Gating strategy of alveolar macrophages (AMs, $CD45^+SigelcF^+F4/80^+CD11b^-CD11c^+$), eosinophils (Eos, $CD45^+SigelcF^+F4/80^+CD11b^+CD11c^-$), and neutrophils (Neut, $CD45^+Gr\text{-}1^{hi}CD11b^{hi}$) in flow cytometry analysis (FACS). **(B)** Influx of eosinophils and neutrophils in mouse lungs upon LPS challenge. **(C)** Total cells, neutrophil**,** and eosinophil count in BALF after LPS instillation. **(D)** Representative images **(left panel)** and semi-quantification **(right panel**, scale bar = 50 μm**)** of Congo red staining of eosinophils (Arrow head) in mouse lungs at 0.5 h after LPS challenge. **(E)** Representative images (**left panel**, scale bar = 100 μm) and semi-quantification **(right panel)** of EPX immunohistochemistry staining (Arrow head) in mouse lungs at 0.5 h after LPS challenge. **(F)** Representative images of transferred eosinophil. Blue, DAPI; Red, TIE2 (endothelial cells); Green, CD45.2 (transferred eosinophils); **Upper panel**, perivascular structure. Intravascular areas were outlined by white dotted lines. **Down panel**, parenchyma and alveoli. Alveolar structure was outlined by white dotted lines. Transferred eosinophils were marked by white arrowheads. Scale bar=5μM. Sample size is marked as individual plots in column images in a single experiment. In semi-quantification of **D** and **E**, each point was the average score of 10-20 random fields of each mouse. Results are representative of 3 independent experiments. *P < 0.05, **P<0.01, ***P<0.001, n.d., not detected.

**Fig. 3 Pulmonary eosinophils are derived from bone marrow and are recruited from peripheral blood upon LPS challenge. (A)** Levels of pulmonary eosinophils in the bone marrow transferred mice. Bone marrow from WT or PHIL mice was transferred into WT or PHIL mice, as shown in the left panel. **(B)** Representative levels of CD45 subtypes of pulmonary eosinophils (FACS plot) and statistical results (column graph) in the bone marrow transferred mice. Bone marrow from CD45.1 mice was transferred into

CD45.2 recipients, as shown in the left panel. **(C)** Representative FACS images and quantified results of eosinophils in blood and lungs of PHIL mice receiving eosinophils at 0.5 h post LPS challenge. $5x10^5$ eosinophils were transferred into PHIL mice by tail vein injection, and the mice were immediately challenged with LPS (left panel). **(D)** Representative FACS images and quantified results of pulmonary CD45.2 eosinophils in CD45.1 WT mice adoptively receiving CD45.2 eosinophils at 0.5 h post LPS challenge. $5x10^5$ eosinophils (CD45.2) from NJ.1638 mice were injected into CD45.1 WT mice through tail vein, and the mice were immediately challenged with LPS (left panel). Sample size is reflected as individual dots in column graphs. Data are representative of 3 independent experiments. *P < 0.05, **P<0.01, ***P<0.001.

**Fig. 4 Loss of eosinophils augments the LPS-induced pulmonary inflammation and injury. (A)** Pulmonary eosinophils and neutrophils detection in LPS-treated WT and PHIL mice by FACS within 2h post LPS injection by FACS. **(B and C)** Total leukocytes and neutrophils **(B)**, CXCL1, and CXCL2 secretion **(C)** in BALF of WT and PHIL mice induced by LPS at early time points. **(D-G)** Levels of pulmonary edema **(D)**, endothelial leakage **(E and F)**, and lung elastance **(G)** were analyzed 24 h after LPS injection. **(H)** Pulmonary inflammation 72 h post LPS instillation (scale bar = 200 μm). **(I)** Eventual mortality of WT and PHIL mice after LPS challenge. Sample size is displayed as individual plots in column graphs. In **G**, N=5. In **I**, N=20. Data are representative of 3 independent experiments. *P < 0.05, **P<0.01, ***P<0.001.

**Fig. 5 CD101 is a marker to distinguish subgroups of eosinophils in both steady phase and allergic milieu. (A)** Scheme of OVA/LPS overlap model. For studying the initiation of ALI, mice were sacrificed 0.5h after LPS administration. **(B)** Amounts of total cells and neutrophils in BALF induced by OVA challenge combined with LPS injection. **(C-D)** Eosinophil subgroups in lung tissue **(C)**, peripheral blood **(D)** and bone marrow **(D)** in OVA-challenged

mice. Representative plots are shown in **C** and **D**, where eosinophils were gated on $CD45^+SiglecF^+CD11c^-$ singlets. **(E)** Cellularity of bone marrow-derived eosinophils **(E** left panel**)** and their CD101 expression **(E** right panel**)**. **(F)** Amount of eosinophils in peripheral blood. **(G)** The expression of CD101 in eosinophils from non-asthma and asthma individuals. In **B**, sample size is marked as individual plots in column graphs. In **C** and **D**, every group consists of 5 individuals. Data are representative of 3 independent experiments except for **F** and **G**. *P < 0.05, **P<0.01, ***P<0.001.

**Fig. 6 $CD101^-$ eosinophils ameliorated, while $CD101^+$ eosinophils exacerbated, the neutrophilic inflammation induced by LPS. (A)** CD101 expression of the aggregated eosinophils in mouse lungs after LPS administration. Left panels, representative images; right panel, quantification results. **(B and C)** Levels of leukocytes and neutrophils **(B)**, and inflammatory cytokines **(C)** in BALF of PHIL mice receiving $CD101^-$ or $CD101^+$ eosinophils at 0.5 h after LPS challenge. **(D-F)** Levels of leukocytes and neutrophils in BALF **(D)**, BALF inflammatory cytokines **(E)**, and representative images of H&E staining (**F** left panel, scale bar = 200 μm) and semi-quantified results (**F** right panel) of PHIL mice receiving $CD101^-$ or $CD101^+$ eosinophils at 24 h after LPS challenge. (**G**) CD101 expression of blood eosinophils in human subjects. HC, healthy controls; ARDS, patients with acute respiratory distress syndrome; PC, positive control (asthma patients). Sample size is marked as individual plots in column graphs. Results are representative of 3 independent experiments except **G**. *P < 0.05, **P<0.01, ***P<0.001.

**Fig. 7 Alox15-mediated Protectin D1 is responsible to the anti-inflammatory effect of $CD101^-$ eosinophils in ALI. (A)** Representative heatmap of RNAseq analysis of differential expression in both $CD101^-$ and $CD101^+$ eosinophils (N=3). **(B-E)** Quantitative PCR analysis of Alox15. **(B)** Expression of Alox15 in $CD101^-$ and $CD101^+$ eosinophils. **(C)** Expression of

Alox15 in lungs during the initiation of LPS-induced ALI. **(D)** Comparison of Alox15 expression between WT and PHIL mice in the initiation of ALI. **(E)** Relative abundance of Alox15 in eosinophils compared to lung tissue. **(F-H)** LC/MS analysis of Protectin D1. **(F)** Identification of Protectin D1. (**G)** Protectin D1 in $CD101^-$ and $CD101^+$ eosinophils. **(H)** Protectin D1 in WT and PHIL mice after 0.5h LPS challenge. Protectin D1-isomer (PDx, 0.05mg/kg) was injected to PHIL mice for continuous 3 days before LPS treatment. **(I)** Amounts of leukocytes and neutrophils in BALF of PHIL mice administrated with Protectin D1-isomer at 0.5h after LPS treatment. Alox15 inhibitor PD146176 was injected intraperitoneally into WT mice at the dose of 10mg/kg 24h before LPS administration. **(J)** Amounts of total leukocytes and neutrophils in BALF 0.5h post LPS challenge. **(K and L)** ALOX15 **(K)** and Protectin D1 **(L)** detection in human eosinophils from both non-asthma patients and asthma patients. Sample size is marked as individual plots in column graphs. Data are triplicate by individual experiments except for **K** and **L**. *P < 0.05, **P<0.01, ***P<0.001.

**Fig. 8. Differential functions of $CD101^-$ and $CD101^+$ eosinophils in ALI pathogenesis.** Homeostatic eosinophils, mainly $CD101^-$, are localized in lung parenchyma. Upon stimulation like LPS or S. aureus, more $CD101^-$ eosinophils are rapidly recruited into the lung, while the factors mediating this early eosinophil recruitment are not clear. These accumulated $CD101^-$ eosinophils attenuate lung inflammation and injury via Alox15-mediated Protectin D1 secretion. On the other side, in allergic microenvironment, $CD101^-$ eosinophils are turned to be positive upon stimulation of certain unknown factors, and the $CD101^+$ eosinophils promote ALI pathogenesis likely through S100a8 or S100a9.

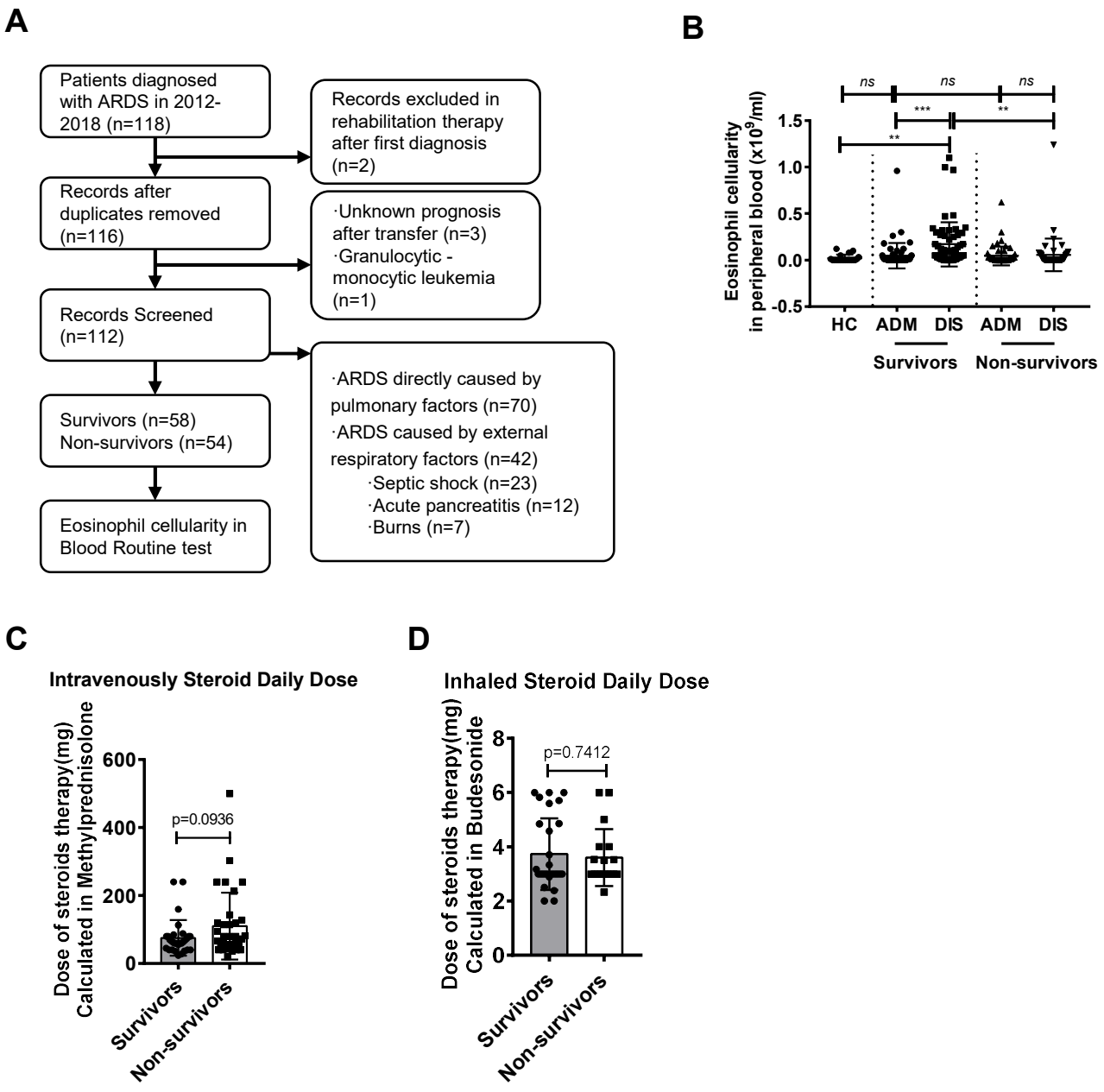
A
Patients diagnosed with ARDS in 2012-2018 (n=118)
Records excluded in rehabilitation therapy after first diagnosis (n=2)
Records after duplicates removed (n=116)
·Unknown prognosis after transfer (n=3)
·Granulocytic - monocytic leukemia (n=1)
Records Screened (n=112)
·ARDS directly caused by pulmonary factors (n=70)
·ARDS caused by external respiratory factors (n=42)
·Septic shock (n=23)
·Acute pancreatitis (n=12)
·Burns (n=7)
Survivors (n=58)
Non-survivors (n=54)
Eosinophil cellularity in Blood Routine test
B
Eosinophil cellularity in peripheral blood (x10^9/ml)
ns
ns
ns
***
**
**
1.5
1.0
0.5
0.0
-0.5
HC
ADM
DIS
ADM
DIS
Survivors
Non-survivors
C
Intravenously Steroid Daily Dose
Dose of steroids therapy(mg) Calculated in Methylprednisolone
600
400
200
0
p=0.0936
Survivors
Non-survivors
D
Inhaled Steroid Daily Dose
Dose of steroids therapy(mg) Calculated in Budesonide
8
6
4
2
0
p=0.7412
Survivors
Non-survivors

**Fig.1**

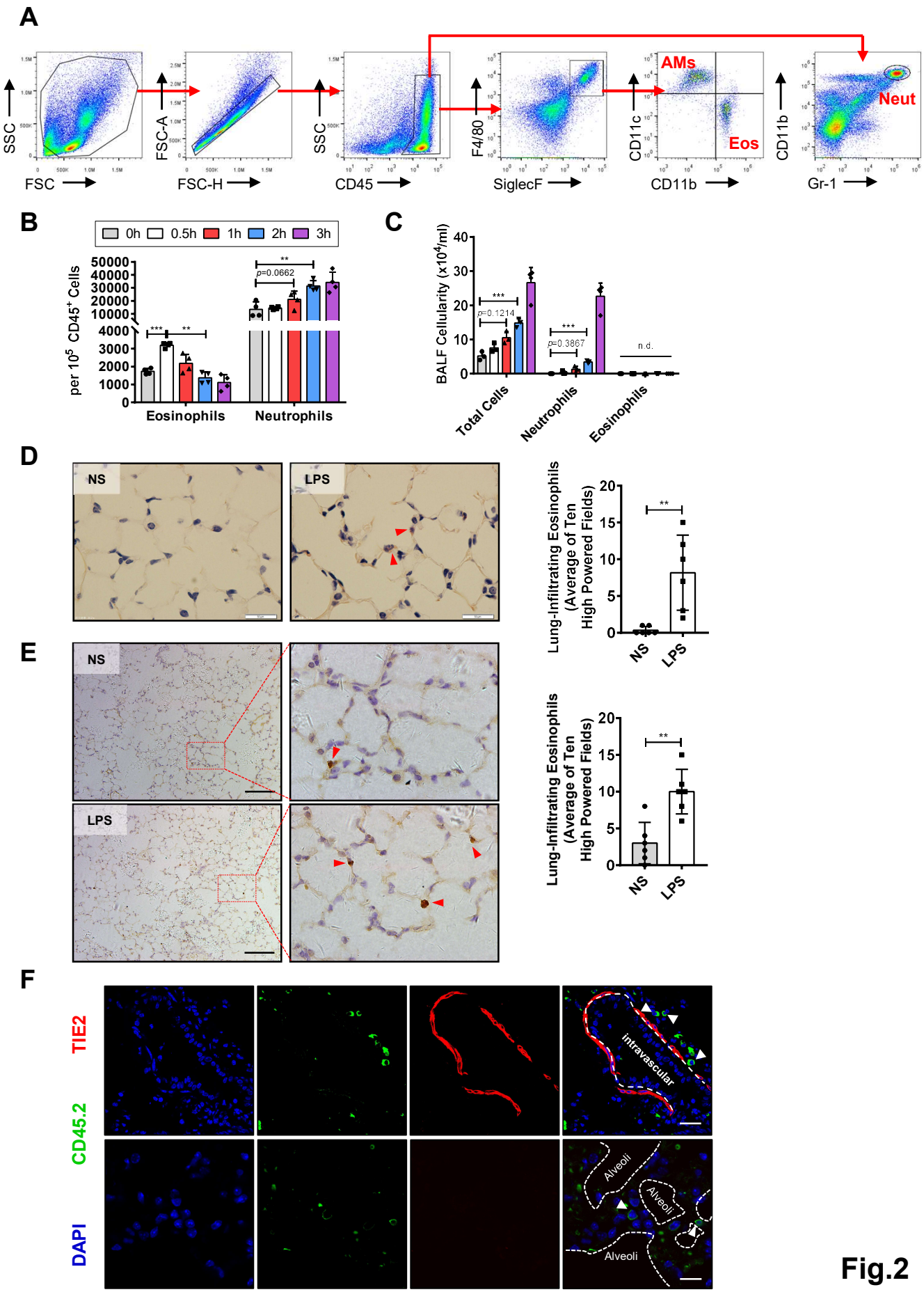
A
SSC
FSC
FSC-A
FSC-H
SSC
CD45
F4/80
SiglecF
CD11c
CD11b
AMs
Eos
CD11b
Gr-1
Neut
B
0h
0.5h
1h
2h
3h
per 10^5 CD45+ Cells
p=0.0662
Eosinophils
Neutrophils
C
BALF Cellularity (x10^4/ml)
p=0.1214
p=0.3867
n.d.
Total Cells
Neutrophils
Eosinophils
D
NS
LPS
Lung-Infiltrating Eosinophils (Average of Ten High Powered Fields)
NS
LPS
E
NS
LPS
Lung-Infiltrating Eosinophils (Average of Ten High Powered Fields)
NS
LPS
F
TIE2
CD45.2
DAPI
Intravascular
Alveoli
Alveoli
Alveoli

Fig.2

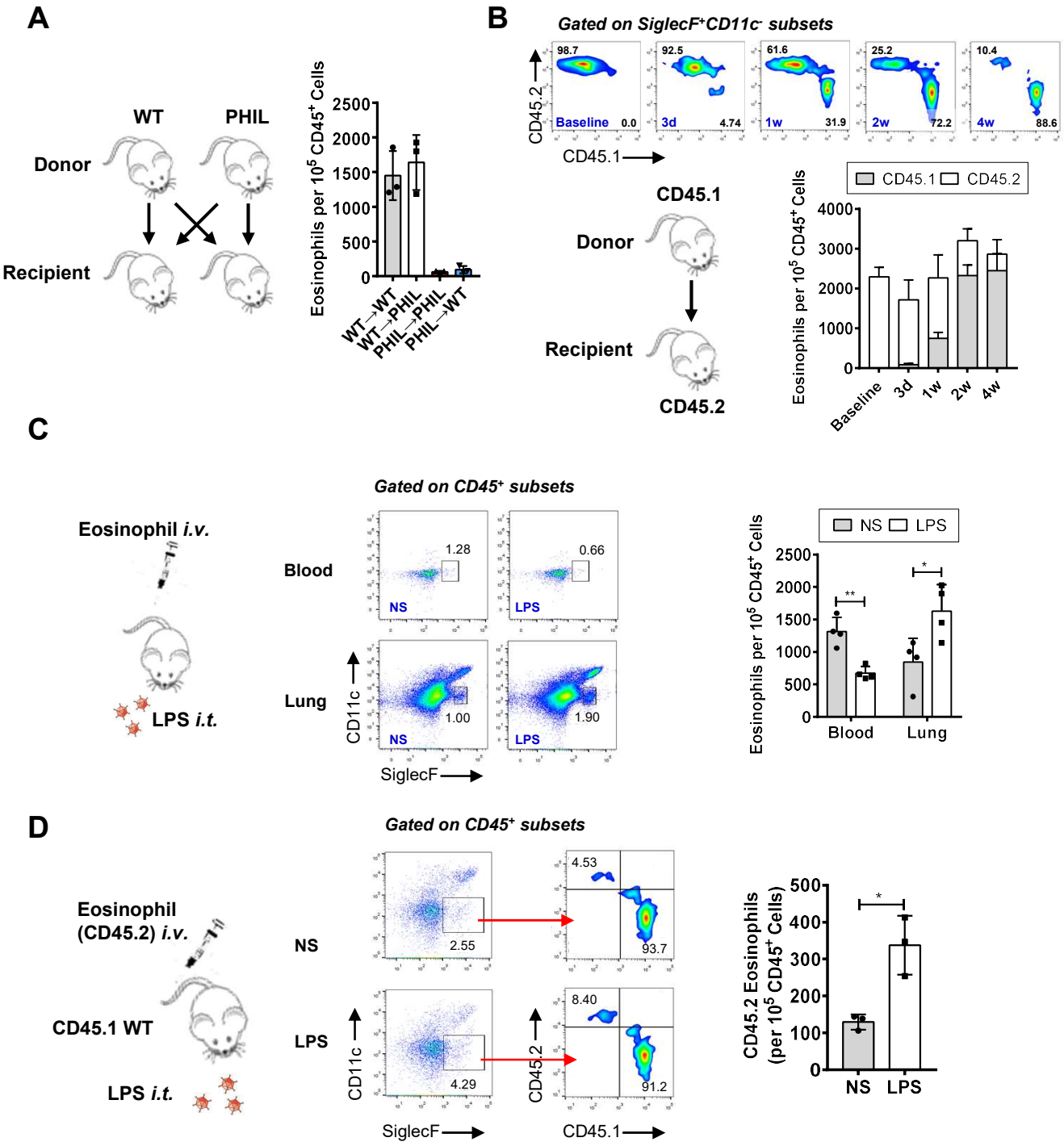
A
WT
PHIL
Donor
Recipient
Eosinophils per 10^5 CD45+ Cells
2500
2000
1500
1000
500
0
WT→WT
WT→PHIL
PHIL→PHIL
PHIL→WT
B
Gated on SiglecF+CD11c- subsets
CD45.2
CD45.1
98.7
Baseline
0.0
92.5
3d
4.74
61.6
1w
31.9
25.2
2w
72.2
10.4
4w
88.6
CD45.1
Donor
Recipient
CD45.2
CD45.1
CD45.2
Eosinophils per 10^5 CD45+ Cells
4000
3000
2000
1000
0
Baseline
3d
1w
2w
4w
C
Gated on CD45+ subsets
Eosinophil i.v.
LPS i.t.
Blood
Lung
1.28
NS
0.66
LPS
1.00
NS
1.90
LPS
CD11c
SiglecF
NS
LPS
Eosinophils per 10^5 CD45+ Cells
2500
2000
1500
1000
500
0
**
*
Blood
Lung
D
Gated on CD45+ subsets
Eosinophil
(CD45.2) i.v.
CD45.1 WT
LPS i.t.
NS
LPS
2.55
4.53
93.7
4.29
8.40
91.2
CD11c
SiglecF
CD45.2
CD45.1
CD45.2 Eosinophils
(per 10^5 CD45+ Cells)
500
400
300
200
100
0
*
NS
LPS

Fig.3

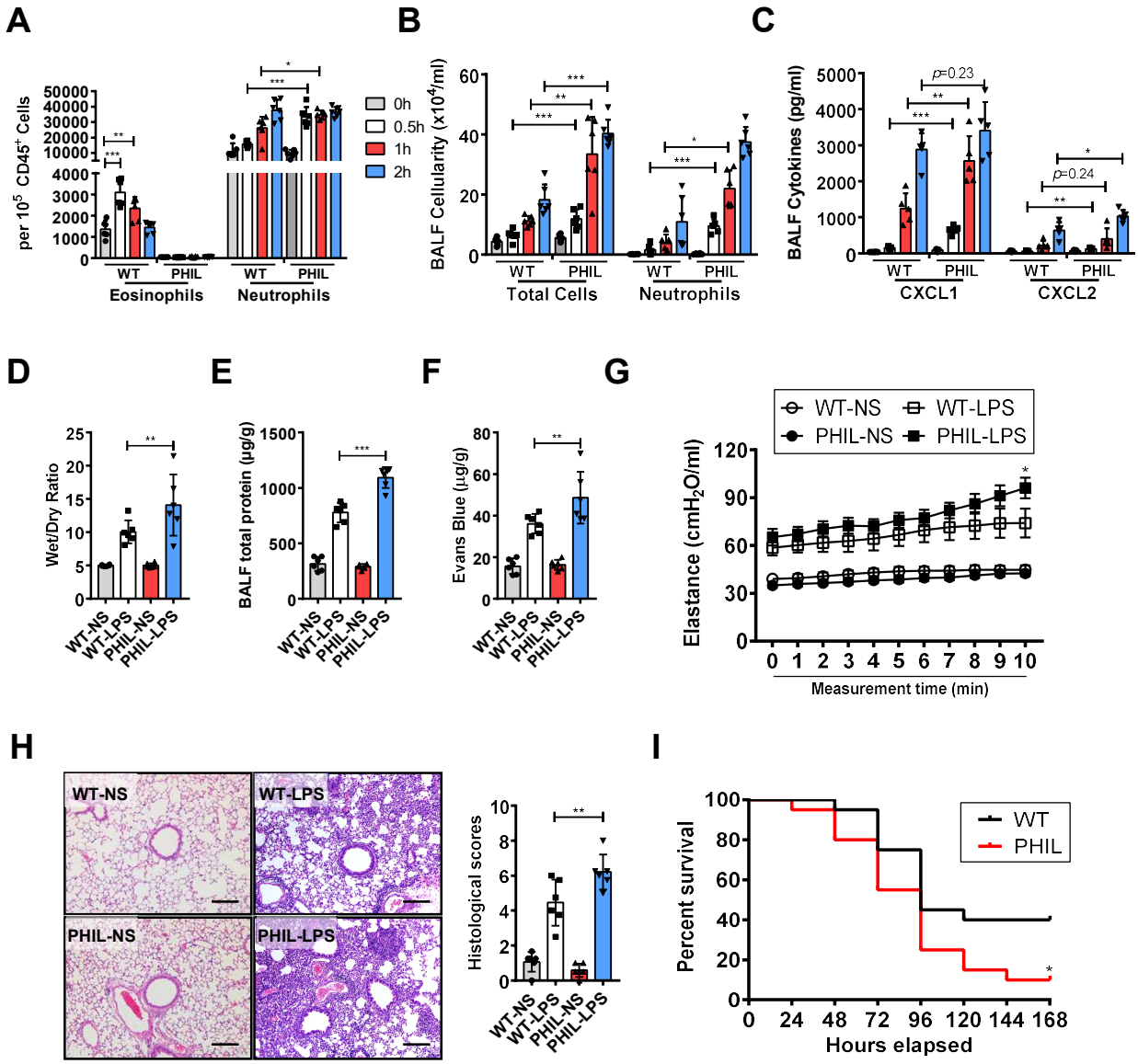
A
B
C
per 10^5 CD45+ Cells
0h
0.5h
1h
2h
WT
PHIL
Eosinophils
Neutrophils
BALF Cellularity (x10^4/ml)
Total Cells
Neutrophils
BALF Cytokines (pg/ml)
p=0.23
p=0.24
CXCL1
CXCL2
D
E
F
G
Wet/Dry Ratio
BALF total protein (μg/g)
Evans Blue (μg/g)
WT-NS
WT-LPS
PHIL-NS
PHIL-LPS
Elastance (cmH2O/ml)
Measurement time (min)
H
I
Histological scores
Percent survival
Hours elapsed

Fig.4

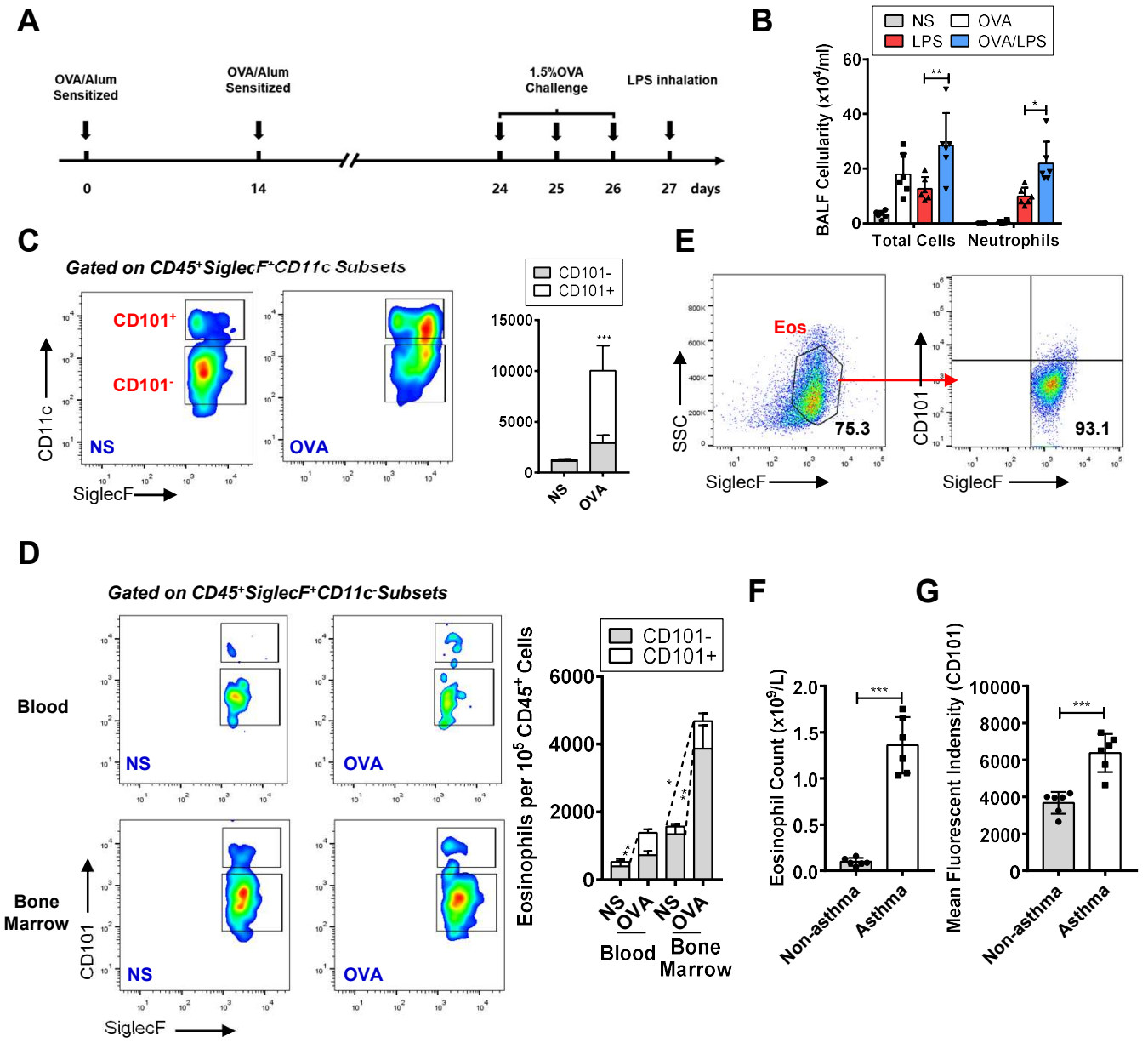
A
OVA/Alum Sensitized
OVA/Alum Sensitized
1.5%OVA Challenge
LPS inhalation
0
14
24
25
26
27 days
B
NS
OVA
LPS
OVA/LPS
BALF Cellularity (x10⁴/ml)
Total Cells
Neutrophils
C
Gated on CD45⁺SiglecF⁺CD11c Subsets
CD101⁺
CD101⁻
NS
OVA
CD11c
SiglecF
CD101-
CD101+
E
Eos
SSC
SiglecF
75.3
CD101
93.1
D
Gated on CD45⁺SiglecF⁺CD11c⁻Subsets
Blood
Bone Marrow
NS
OVA
CD101
SiglecF
Eosinophils per 10⁵ CD45⁺ Cells
F
Eosinophil Count (x10⁹/L)
Non-asthma
Asthma
G
Mean Fluorescent Indensity (CD101)
Non-asthma
Asthma

Fig.5

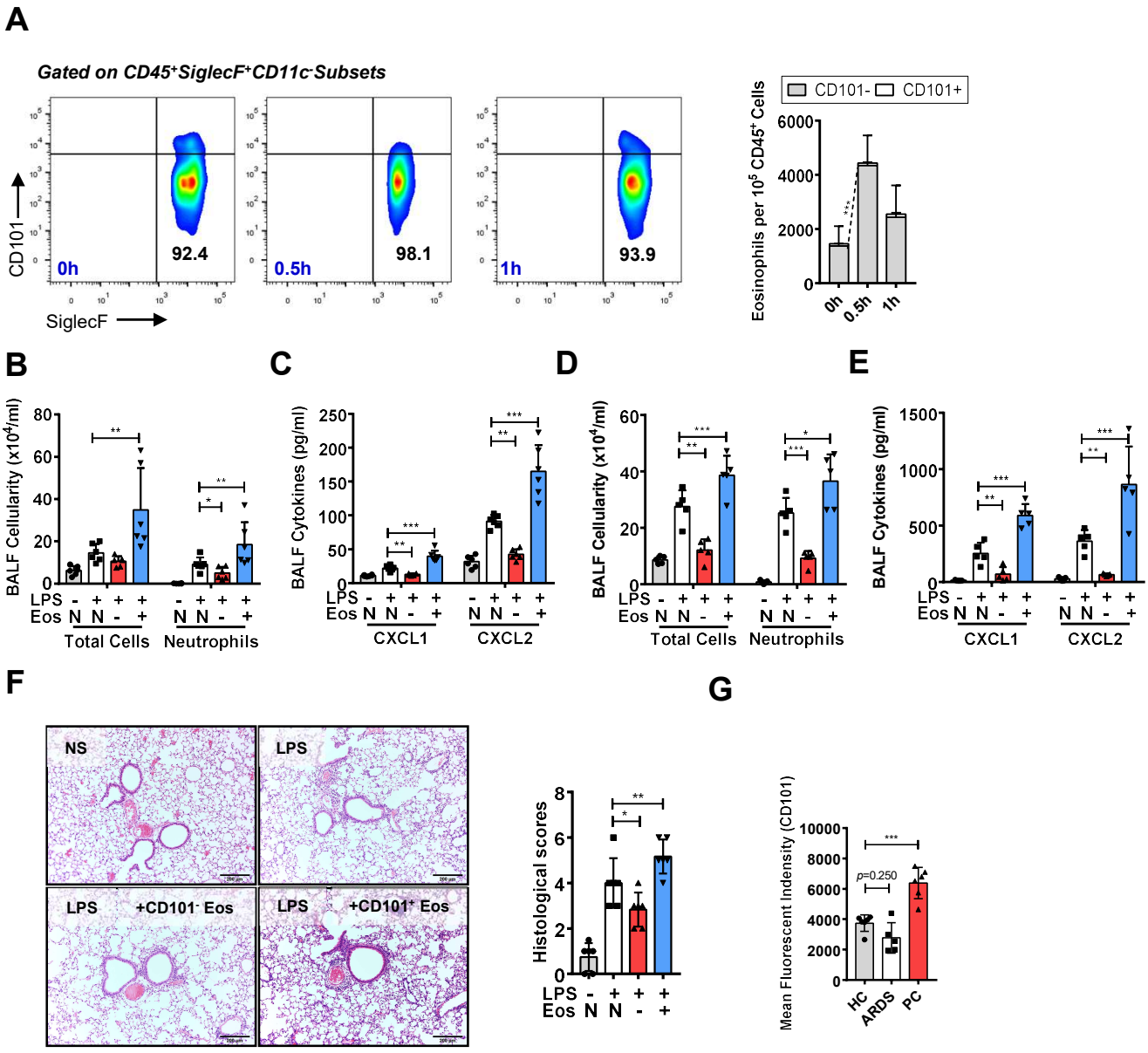
A
Gated on CD45+SiglecF+CD11c- Subsets
CD101
SiglecF
0h
92.4
0.5h
98.1
1h
93.9
CD101- CD101+
Eosinophils per 10^5 CD45+ Cells
B
BALF Cellularity (x10^4/ml)
LPS
Eos
Total Cells
Neutrophils
C
BALF Cytokines (pg/ml)
CXCL1
CXCL2
D
BALF Cellularity (x10^4/ml)
Total Cells
Neutrophils
E
BALF Cytokines (pg/ml)
CXCL1
CXCL2
F
NS
LPS
LPS +CD101- Eos
LPS +CD101+ Eos
G
Histological scores
Mean Fluorescent Indensity (CD101)
p=0.250
HC
ARDS
PC

Fig.6

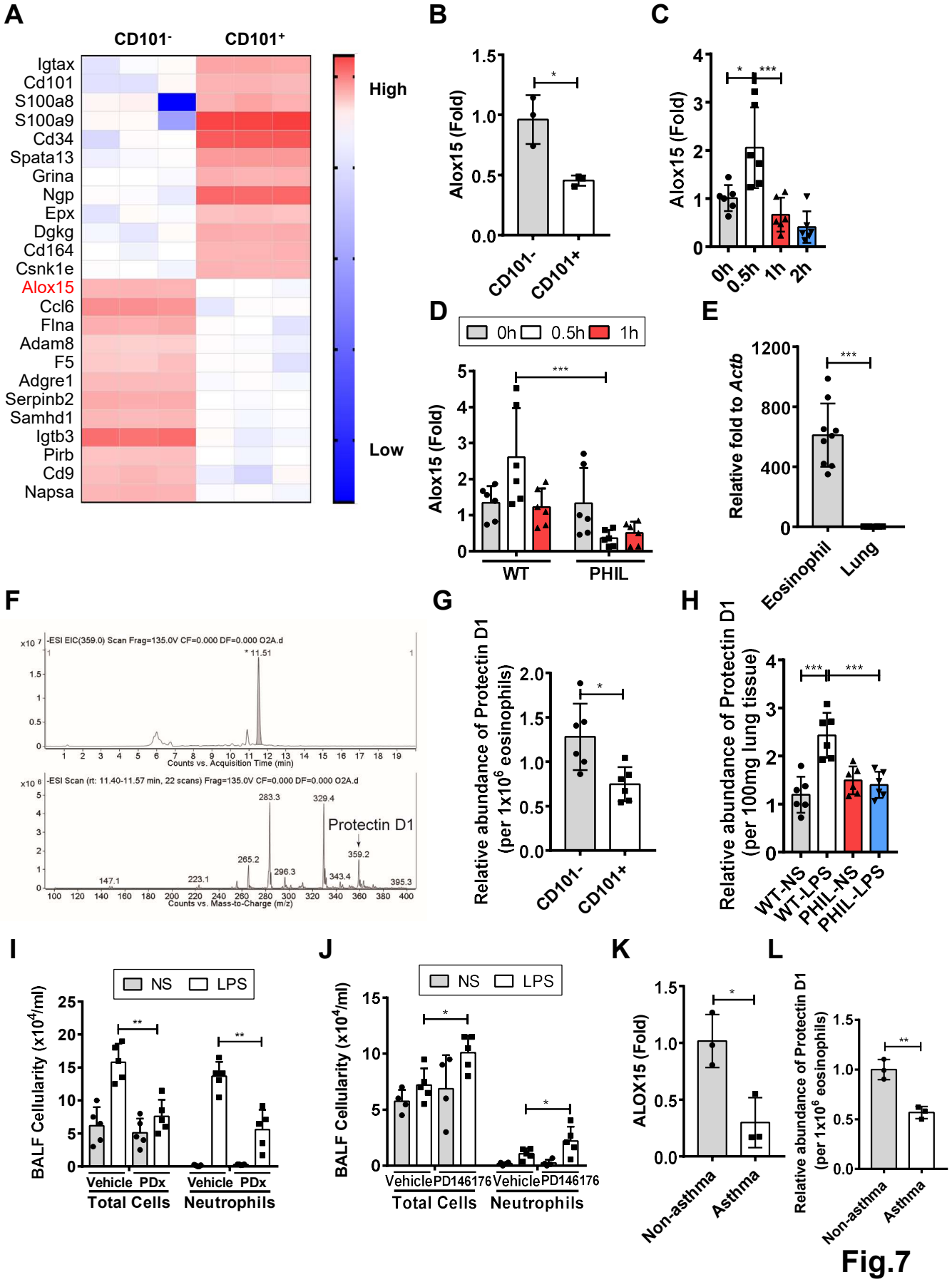
A
CD101-
CD101+
Igtax
Cd101
S100a8
S100a9
Cd34
Spata13
Grina
Ngp
Epx
Dgkg
Cd164
Csnk1e
Alox15
Ccl6
Flna
Adam8
F5
Adgre1
Serpinb2
Samhd1
Igtb3
Pirb
Cd9
Napsa
High
Low
B
Alox15 (Fold)
CD101-
CD101+
C
Alox15 (Fold)
0h
0.5h
1h
2h
D
0h
0.5h
1h
Alox15 (Fold)
WT
PHIL
E
Relative fold to Actb
Eosinophil
Lung
F
-ESI EIC(359.0) Scan Frag=135.0V CF=0.000 DF=0.000 O2A.d
Counts vs. Acquisition Time (min)
-ESI Scan (rt: 11.40-11.57 min, 22 scans) Frag=135.0V CF=0.000 DF=0.000 O2A.d
Protectin D1
Counts vs. Mass-to-Charge (m/z)
G
Relative abundance of Protectin D1 (per 1x10^6 eosinophils)
CD101-
CD101+
H
Relative abundance of Protectin D1 (per 100mg lung tissue)
WT-NS
WT-LPS
PHIL-NS
PHIL-LPS
I
NS
LPS
BALF Cellularity (x10^4/ml)
Vehicle
PDx
Total Cells
Neutrophils
J
NS
LPS
BALF Cellularity (x10^4/ml)
Vehicle
PD146176
Total Cells
Neutrophils
K
ALOX15 (Fold)
Non-asthma
Asthma
L
Relative abundance of Protectin D1 (per 1x10^6 eosinophils)
Non-asthma
Asthma

Fig.7

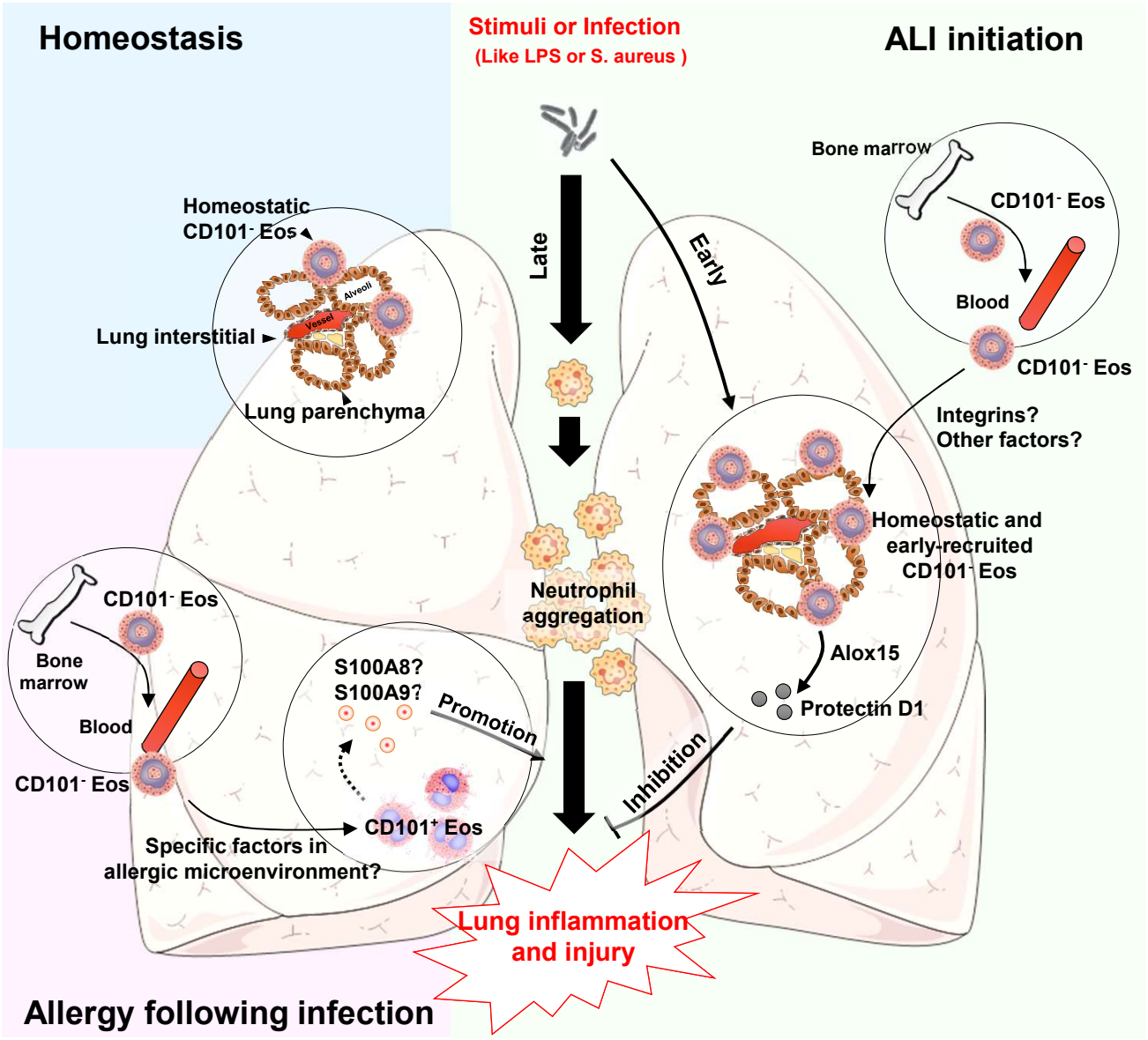
Homeostasis
Stimuli or Infection
(Like LPS or S. aureus )
ALI initiation
Homeostatic
CD101- Eos
Alveoli
Vessel
Lung interstitial
Lung parenchyma
Late
Early
Bone marrow
CD101- Eos
Blood
CD101- Eos
Integrins?
Other factors?
Homeostatic and
early-recruited
CD101- Eos
Neutrophil
aggregation
Alox15
Protectin D1
CD101- Eos
Bone
marrow
Blood
CD101- Eos
S100A8?
S100A9?
Promotion
Inhibition
CD101+ Eos
Specific factors in
allergic microenvironment?
Lung inflammation
and injury
Allergy following infection

Fig.8

**Supplementary Materials**

# Homeostatic and Early Recruited CD101$^{-}$ Eosinophils Suppress Endotoxin-induced Acute Lung Injury

Chen Zhu, MD, PhD,[a,#] Qing-Yu Weng, MD,[a,#] Ling-Ren Zhou, MD,[a,#] Chao Cao, MD, PhD,[b] Fei Li, MD, PhD,[a] Yin-Fang Wu, MD, PhD,[a] Yan-Ping Wu, MD, PhD,[a] Miao Li, MD, PhD,[a] Yue Hu, MD, PhD,[a] Jia-Xin Shen, MD,[a] Xue-Fang Xiong, MD,[a,c] Fen Lan, MD, PhD,[a] Li-Xia Xia, MD, PhD,[a] Bin Zhang, MD,[a] Hao Zhang, MD, PhD,[a] Man Huang, MD, PhD,[d] Song-Min Ying, MD, PhD,[a] Hua-Hao Shen, MD, PhD,[a,e,*] Zhi-Hua Chen, PhD,[a,*] Wen Li, MD, PhD,[a,*]

[a]Key Laboratory of Respiratory Disease of Zhejiang Province, Department of Respiratory and Critical Care Medicine, Second Affiliated Hospital of Zhejiang University School of Medicine, Hangzhou, Zhejiang, 310009, China;

[b]Department of Respiratory Medicine, Ningbo First Hospital, Ningbo, Zhejiang, 315000, China;

[c]Department of Respiratory Medicine, The Central Hospital of Lishui City, Lishui, Zhejiang, 323001, China;

[d]Department of Central Intensive Care Unit, Second Affiliated Hospital of Zhejiang University School of Medicine, Hangzhou, Zhejiang, 310009, China;

[e]State Key Lab for Respiratory Diseases, Guangzhou, Guangdong, 510120, China.

Authorship note:

[#]These authors contributed equally to this article.

[*]Correspondence should be addressed to W.L. (liwen@zju.edu.cn), Z.H.C. (zhihuachen@zju.edu.cn) or H.H.S. (huahaoshen@zju.edu.cn)

**Methods**

*Mice.* NJ.1638 mice and PHIL mice were generously provided by Prof. James Lee at Mayo Clinic, AZ. WT CD45.2 C57BL/6 mice were purchased from Shanghai SLAC laboratory animal Co., Ltd, while WT CD45.1 C57BL/6 mice were generously gifted from Prof. Lie Wang at Institute of Immunology, Zhejiang University School of Medicine. All the strains above were housed and bred in Laboratory Animal Center of Zhejiang University, Hangzhou, China. All experimental protocols were approved by the Ethical Committee for Animal Studies at Zhejiang University.

ALI was induced by injection of 20 mg/kg LPS (from *E. Coli* O55:B5, Sigma) or $1x10^7$ CFU *S. aureus* intratracheally (*i.t.*). For observing the initiation of inflammation, mice were sacrificed 30 mins after LPS instillation. For detecting eventual ALI, mice were euthanized 24 hours and above after LPS injection. For surviving curve, ALI mice were observed until day 7, and the decline of body weight more than 20% compared to their initial weight, was regarded as biologically dead[1]. For lung function assessment[2, 3], ALI mice were ventilated by Buxco Finepointe system, and dynamic lung compliance (reciprocal of elastance) was recorded until 10 min.

The establishment of ovalbumin (OVA, Sigma)-induced allergic airway inflammation model was fully described elsewhere[4, 5].

For bone marrow transfer, recipient mice were first received X-ray radiation at the dose of 8 Gy for the clearance of hematopoietic stem cells, and $1x10^7$ whole bone marrow derived cells from donor mice were injected through tail veins. Chimera mice were further analyzed at indicated time points after bone marrow transplant.

All the mice involved in LPS or OVA models were allocated randomly.

*Human subjects.* Patients with ARDS were identified according to the guidelines for the diagnosis and treatment of acute lung injury/acute respiratory distress syndrome (diagnosed by Congress of Chinese Society of

Critical Care Medicine, which shows no differences in the diagnosis of ARDS comparing with ATS/ESICM/SCCM guideline). All ARDS inpatients were enrolled in The Second Affiliated Hospital of Zhejiang University, School of Medicine from 2012 to 2018. The observation was based on the circulated eosinophil counts when hospitalized (within 24 hours after hospitalization) and when discharged (within 24 hours before discharge or death). Sex- and age-matched healthy subjects were enrolled as baseline controls. No differences were determined in age and sex between survivor group and non-survivor group (Table S1). This study was approved by the ethics committees of The Second Affiliated Hospital of Zhejiang University, School of Medicine.

*Mouse behavioral score.* Mice were scrutinized and assessed every day after LPS endotracheal injection. Scores were assigned on the basis of physical appearance and activity[6]. The behavioral score was calculated by four categories: a) Coat, 1 (smooth), 2 (slight perturbing), 3 (apparent perturbing); b) Activity, 1 (vivacious), 2 (idle), 3 (sedentary), 4 (fixed); c) Respiration, 1 (natural), 2 (toilsome), 3 (labored and irregular); d) Posture, 1 (unfolded), 2 (huddled). The scores of four aspects add up to the total score from 4 to 12.

*Reagent.* Liposaccharides from *E. coli* (O55:B5), Grade V ovalbumin and Evans blue dye were purchased from Sigma-Aldrich. EPX antibody was a generous gift from Prof. J.J Lee. Mouse CXCL-1 and CXCL-2 Elisa Kit were purchased from R&D and were performed according to manufacturer's protocols. Protectin D1-isomer (PDx) and PD146176 was purchased from Cayman Chemical.

*Eosinophil isolation from NJ.1638 mice.* Eosinophils were isolated from peripheral blood of NJ.1638 mice[7]. Briefly, peripheral blood from NJ.1638 mice was layered onto percoll (GE healthcare) gradient. The eosinophils

containing contaminant cells were further purified with $CD4^{-}CD8^{-}B220^{-}Ter119^{-}$ magnetic beads (Miltenyi Biotec) isolation afterwards. The purity of eosinophils was about 95%.

*Human eosinophils detection and purification.* For detection of CD101 expression in human eosinophils, peripheral blood samples were obtained from ARDS, asthmatic, or non-asthmatics enrolled in Second affiliated hospital of Zhejiang University, School of medicine (Hangzhou, China) or Ningbo First Hospital (Ningbo, China). All human samples were Chinese Han population without systemically or inhaled steroid therapy. The asthmatic patients were diagnosed by bronchial provocation test. All the procedures are authorized by the Ethics committee of Second affiliated hospital of Zhejiang University, School of Medicine (approval no. 2016008 to Wen Li) and Ethics committee of Ningbo First Hospital (approval no. 2016-R017 to Chao Cao). All the participants had been notified the consensus to their involvement in the study, and all the samples are treated after anonymization. Brief information of each patient was summarized as Table S2 and Table S3.

Human eosinophils from healthy subjects and asthmatic patients were purified from peripheral blood. Briefly, erythrocytes was lysed by red blood lysis solution (BD Pharmingen). Next, the harvested cells were resuspended and layered onto 60% percoll gradient of equal volume, and centrifuged at 800 g for 30 min in a density gradient pattern to obtain leukocyte compartment. Leukocytes were incubated with APC-conjugated Siglec-8 antibody and then with Anti-APC MicroBeads (Miltenyi Biotic) for another 30 min. Eosinophils were then purified by Siglec-8 positive selection using magnetic beads isolation.

*Liquid culture and colony forming assay of bone-marrow-derived-eosinophils.* The protocols were detailed described elsewhere[4, 8]. For liquid culture, non-adherent mononuclear cells at the concentration of $1x10^{6}$/ml were seeded

in IMDM complete medium including 20% fetal bovine serum (Gibco), with 100 IU/ml penicillin mixed with 10 mg/ml streptomycin, 2mM L-glutamine (Sigma-Aldrich), 1mM sodium pyruvate (Sigma-Aldrich), 1x non-essential amino acids (Sigma-Aldrich), 0.006‰ 2-ME (Sigma-Aldrich), Flt-3L (100 ng/ml, Peprotech), and SCF (100 ng/ml, Peprotech) were added into culture medium for the first 4 days. The culture medium was replaced with recombinant interleukin 5 (IL-5, 10 ng/ml, R&D) in day 4 and day 8 thereafter. For colony forming assay, $2x10^5$ bone-marrow-derived-non-adherent mononuclear cells or sorted eosinophils were seeded in IMDM completed medium containing 0.9% methylcellulose (Stem Cell) in the presence of IL-5 (10 ng/ml), and the colonies were identified on day 7.

*Lung single cell suspension harvest and Flow Cytometry.* Mice were euthanized by pentobarbital anesthetization, and lungs were perfused by 10 ml PBS through right ventricle injection to minimize the interference with trapped leukocytes in circulation. Ambilateral lungs were harvested and cut into pieces, and were digested by 1 mg/ml collagenase I (Sigma) for 90 mins. Finally, digested tissues were filtered to obtain single cell suspension.

For flow cytometric analysis (FACS), Cytoflex (Beckman Coulter) was used to identify cell surface markers. Cell sorting were performed by Moflo Astrios EQ (Beckman Coulter). All the results were analyzed by Flowjo X software (Treestar). Fluorescence conjugated antibodies were listed as Table S4. The corresponding isotype control antibodies were purchased from Biolegend and used in the staining of flow cytometry analysis.

For BrdU or EdU staining, the processes were according to manufactures' protocols (BD Pharmingen). *In vivo*, BrdU solution at the dose of 10 mg/ml in sterile 1X PBS was injected to WT mice intraperitoneally, and each mouse was received 200 μl (2mg) BrdU. Meanwhile, BrdU was diluted into 0.8 mg/ml in drinking water to keep the intake of BrdU. Mice were sacrificed and analyzed 24h after intraperitoneal injection. *In vitro*, a final concentration of 10 μM EdU

was treated for 2h. The process of staining and detecting was performed in terms of the manual of corresponding kit.

*Lung histology and immunofluorescence assay.*

. Paraformaldehyde-fixed and paraffin-embedded lung tissues were cut perpendicular to small airways to embody their structures and peripheries of both large and small airways at the same time according to previous reports[9, 10]. For eosinophils detection, Congo red staining[11] and EPX immunohistochemistry staining were performed to distinguish eosinophils in lung parenchyma. For inflammation and injury assessment, H&E staining was performed. Stained slices were visualized by Olympus BX51 microscope equipped with 4/0.3 NA objective and DP70 digital camera. The inflammatory score was calculated as following features[6]: lung interstitial edema, haemorrhage, and neutrophil infiltration. Each feature could be assessed a score of 0 (no injury), 1 (limited injury), 2 (visible injury) and 3 (severe injury). The scores of three aspects add up to the total score from 0 to 9.

For immunofluorescence assay, lung tissue sections were stained with anti-TIE2 (as endothelial cells, Servicebio) and anti-CD45.2 (as transferred eosinophils, Invitrogen) according to manufacturer's instruction. Fluorescence images were captured by Olympus IX83-FV3000-OSR confocal microscope.

*RNA isolation and quantitative PCR*. Eosinophils or lung tissues were lysed by RNAiso reagent (Takara, Japan) as stated by manufacturer's protocol. Primers involved in real-time PCR were manufactured by Shanghai Bioengineering (Shanghai, China). Reverse transcription and real-time PCR were performed using PrimeScript TM RT-PCR kit (Takara) and SYBR Primix TaqTM (Takara), respectively. Primers used were listed below:

*Alox15*: forward, 5'-GGCTCCAACAACGAGGTCTAC-3'; reverse, 5'-AGGTATTCTGACACATCCACCTT-3';

*Actb*: forward, 5'-AGAGGGAAATCGTGCGRGAC-3'; reverse,

5’-CAATAGTGACCTGGCCGT-3’.

*ALOX15*: forward, 5’- GGGCAAGGAGACAGAACTCAA-3’; reverse, 5’-CAGCGGTAACAAGGGAACCT-3’;

*ACTB*: forward, 5’- CATGTACGTTGCTATCCAGGC-3’; reverse, 5’-CTCCTTAATGTCACGCACGAT-3’.

The relative abundance was analyzed in delta-delta CT method and normalized to *Actb* or *ACTB*.

*RNAseq*. Eosinophils both $CD101^-$ and $CD101^+$ were isolated from OVA-induced asthmatic NJ.1638 mice by flow cytometric sorting system. The samples were disposed and analyzed by BGI (Shenzhen). RNAseq data had been uploaded in NCBI under BioProject ID: PRJNA479696 (http://www.ncbi.nlm.nih.gov/bioproject/479696)

*LC/MS Analysis of Protectin D1.* The protocol of lipid extraction and LC/MS analysis were abundantly described elsewhere[12, 13]. Briefly, lung tissues or eosinophils were lysed by the solution including PBS, methanol and chloroform (1:1:2). The mixture was fully vortexed then centrifuged at 2200 g for 6 mins. The organic phase was collected and dried under nitrogen flushing, followed by 50 μl methanol re-suspension[13].

For *in vitro* experiments, $1x10^6$ eosinophils were stimulated by 2 μM $Ca^{2+}$ ionophore A23187 (Sigma) and 10 μM DHA (Sigma) for 30 minutes at 37℃. The incubation was suspended with 2 volumes of ice-cold methanol and lipid was extracted as previous described[14].

The LC/MS analysis was by an Agilent 6400 Series Triple Quadrupole LC/MS System. Protectin D1 was identified as *m/z* = 359 and acquisition time approach to 11.5 min by published criteria[12] and monitored by ESI ionization mode. As lacking of commercial standard of Protectin D1, production of Protectin D1 was represented as relative expression rather than quantification. The assay was performed by Analysis Center of Agrobiology and

Environmental Sciences, Zhejiang University.

**Figure Legends**

**Fig. S1 Simplified gating strategy of pulmonary eosinophils.** Gating strategy of eosinophils (Eos, $CD45^+SiglecF^+CD11c^-$) and alveolar macrophages ($CD45^+SiglecF^+CD11c^+$).

**Fig. S2 Amount of pulmonary eosinophils in homeostasis.** The comparison between the number of pulmonary eosinophils with that of AMs **(A)** and that of circulated eosinophils **(B)**. ***P<0.001.

**Fig. S3 Morphology of BALF leukocytes after LPS injection.** Representative images of Wrights-Giemsa staining of BALF leukocytes upon LPS administration by cytospin. Legend of morphology was represented by BALF leukocyte cytospin of OVA-induced model. Alveolar macrophages, black arrowheads. Eosinophils, orange arrowheads. Neutrophils, Blue arrowheads. Scale bar = 50μm.

**Fig. S4 Early induction of pulmonary eosinophils by *S. aureus.* (A, B)** Influx of eosinophils **(A)** and neutrophils **(B)** by flow cytometry analysis within 2 h post $1x10^7$ CFU *S. aureus* intratracheal injection. *P < 0.05.

**Fig. S5 Distribution of transferred eosinophils without ventricle flushing.** Representative immunofluorescence images of transferred CD45.2 eosinophils in lung without flush. Blue, DAPI; Red, TIE2 (endothelial cells); Green, CD45.2 (transferred eosinophils). Intravascular areas were outlined by white dotted lines. Extravascular transferred eosinophils and intravascular eosinophils were marked by white arrowheads. Scale bar=5μM.

**Fig. S6 Depletion of pulmonary eosinophils in PHIL mice.** Pulmonary

eosinophils detection in lung suspension of WT and PHIL mice.

**Fig. S7 Repopulation of AMs in chimera mice.** The establishing scheme of chimera mice was as Fig.3B. CD45 subtypes of AMs and eosinophils.

**Fig. S8 Expression of eotaxin in lungs post LPS administration. (A)** mRNA level in lung homogenate within 2h after LPS instillation. **(B and C)** Eotaxin ELISA in BALF **(B)** and lung homogenate **(C)** after LPS challenge.

**Fig. S9 Proliferative ability of local eosinophils. (A)** BrdU expression in pulmonary eosinophils (left panel) and circulating monocytes (right panel). **(B)** EdU expression in sorted eosinophils and Eol-1 cells. **(C)** Colony forming units in pulmonary eosinophils (left panel) and bone-marrow-derived non-adherent mononuclear cells (right panel).

**Fig. S10 Pulmonary inflammation and individual status 24h after LPS injection.** ALI mice were established and analyzed 24h after LPS administration. **(A and B)** Pulmonary inflammatory level. Total leukocyte and neutrophil amount **(A)** and inflammatory cytokines **(B)**. **(C and D)** individual status. Body weight decline **(C)** and behavior assessment score **(D)**. *P < 0.05, **P<0.01. ***P<0.001.

**Fig. S11 Exacerbation of pulmonary inflammation in PHIL mice after *S. aureus* infection.** BALF total cell count and neutrophils cellularity of PHIL mice after *S. aureus* exposure. *P < 0.05, **P<0.01.

**Fig. S12 Eosinophil infiltration in OVA-induced allergic airway inflammation.** Allergic airway inflammation in OVA-induced mouse model. **(A)** Eosinophil count in BALF. **(B)** Representative images of EPX-IHC in mouse

lungs in OVA models.

**Fig. S13 CD101 expression in circulating eosinophils in LPS model.** CD101 expression in blood eosinophils after 0.5h treatment of LPS in mice. ns, no significance.

**Fig. S14 CD101 expression in eosinophils after different treatment.** CD101 expression in eosinophils after 24h treatment of interleukin-3 (IL-3, 10ng/ml), interleukin-5 (IL-5, 10ng/ml), granulocyte-macrophage colony stimulating factor (GM-CSF, 10ng/ml) and HDM (10μg/ml). Null, control groups. Positive, sorted $CD101^+$ eosinophils. ns, no significance, ***P<0.001.

**Fig. S15 Subtypes of early-induced eosinophils in *S. aureus* model.** CD101 expression of the aggregated eosinophils in mice lungs after $1x10^7$ *S.aureus* administration. Representative image, upper panels; quantification, nether panel. *P < 0.05.

**Fig. S16 Efficacy of eosinophil adoptive transfer.** NJ.1638 derived eosinophils ($5x10^5$ in 50μl) were transferred into WT or PHIL mice. WT or PHIL mice who received saline only (Eos-Null) were set as control. Pulmonary eosinophils assessment by flow cytometry.

**Fig. S17 Inflammatory response of eosinophil subsets post LPS treatment.** Two subgroups of pulmonary eosinophils were purified by FACS sorting system. Expression of TLR4 and Myd88 signaling, and expression of inflammatory cytokines.

**Fig. S18 Prevention and resolution models in eosinophil deficiency mice.** Prevention model (A-C) was schemed in A. B, BALF total cells, C, neutrophils. Resolution model (D-F) was schemed in D. E, BALF total cells, F, neutrophils.

**Table S1. Brief characteristics of ARDS inpatients. (In Fig. 1)**

| | Healthy Controls | Survivors | Non-survivors | P-Value (Survivors vs. Non-survivors) |
|---|---|---|---|---|
| Number | 20 | 58 | 54 | - |
| Age, yrs | 54.2±11.1 | 52.9±16.4 | 55.7±15.8 | 0.37 |
| Sex (M/F) | 15/5 | 46/12 | 41/13 | - |
| Blood eosinophils ($x10^9$/L) 24h within hospitalization | 0.020±0.037 | 0.046±0.018 | 0.046±0.014 | 0.97 |

Data are presented as means ± SD. Categorical variables in patients' information were analyzed by Pearson's chi square tests where $P<0.05$ is considered significant.

**Table S2. Brief information of asthmatic patients and non-asthmatic control. (In Fig. 5 and Fig. 7)**

| | Non-asthma | Asthma |
|---|---|---|
| Sex (M/F) | 3/3 | 3/3 |
| Age, yrs | 44.67±11.02 | 46.33±14.17 |
| Eosinophil ($x10^9$/ml) | 1.80±0.32 | 14.45±4.28 |
| Diagnosis constitution (Count) | Healthy (1)<br>Upper airway cough syndrome (1)<br>Chronic cough (1)<br>Pneumonia after treatment (3) | Asthma exacerbation (4)<br>Asthma with ABPA (1)<br>Cough variant asthma (1) |

Data are presented as means ± SD. Categorical variables in patients' information were analyzed by Pearson's chi square tests where $P<0.05$ is considered significant.

**Table S3. Brief information of ARDS patients. (In Fig. 6)**

| No. | Sex | Age | Primary diagnosis |
|---|---|---|---|
| 1 | M | 55 | Myocardial infarction |
| 2 | M | 53 | Subarachnoid hemorrhage |

| | | | |
|---|---|---|---|
| 3 | M | 67 | Severe pneumonia |
| 4 | M | 77 | Peritonitis |
| 5 | F | 69 | Meningioma |

**Table S4. Fluorescent antibodies used in the experiments.**

| Target | Fluorescent | Manufacturer | Clone | Cata. No. |
|---|---|---|---|---|
| Mouse CD45 | FITC | Biolegend | 30-F11 | 103107 |
| Mouse CD45 | BV510 | Biolegend | 30-F11 | 103138 |
| Mouse SiglecF | PE | BD Pharmingen | E50-2440 | 552126 |
| Mouse F4/80 | Pe-Cy7 | eBioscience | BM8 | 25-4801-82 |
| Mouse CD11b | FITC | Biolegend | M1/70 | 101205 |
| Mouse CD11b | BV421 | Biolegend | M1/70 | 101251 |
| Mouse CD11c | FITC | eBioscience | N418 | 11-0114-82 |
| Mouse CD11c | APC | eBioscience | N418 | 17-0114-82 |
| Mouse CD45.1 | Pacific Blue | Biolegend | A20 | 110721 |
| Mouse CD45.2 | FITC | Biolegend | 104 | 109805 |
| Mouse CD101 | Pe-Cy7 | eBioscience | Moushi101 | 25-1011-82 |
| Mouse Gr-1 | BV421 | Biolegend | RB6-8C5 | 108445 |
| Mouse CD115 | PE | eBioscience | 12-3A3-1B10 | 12-1159-41 |
| Mouse Ki-67 | PerCP-Cy5.5 | Biolegend | 16A8 | 652423 |
| Mouse CD4 | Biotin | Biolegend | GK1.5 | 100403 |
| Mouse CD8a | Biotin | Biolegend | 53-6.7 | 100703 |
| Mouse B220 | Biotin | Biolegend | RA3-6B2 | 103203 |
| Mouse Ter119 | Biotin | Biolegend | Ter-119 | 116203 |
| Human Siglec-8 | APC | Biolegend | 7C9 | 347105 |
| Human CCR3 | BV510 | Biolegend | 5E8 | 310721 |
| Human CD101 | PE | Biolegend | BB27 | 331011 |
| Human CD45 | Pe-Cy7 | Biolegend | 2D1 | 368532 |
| BrdU | APC | BD Pharmingen | Kit Catalog #552598 | |
| EdU | FITC | BD Pharmingen | Kit Catalog #565455 | |

**Reference**


1. Hu Y, Lou J, Mao YY, Lai TW, Liu LY, Zhu C, Zhang C, Liu J, Li YY, Zhang F, Li W, Ying SM, Chen ZH, Shen HH. Activation of MTOR in pulmonary epithelium promotes LPS-induced acute lung injury. *Autophagy* 2016: 12(12): 2286-2299.

2. Gotts JE, Bernard O, Chun L, Croze RH, Ross JT, Nesseler N, Wu X,

Abbott J, Fang X, Calfee CS, Matthay MA. Clinically relevant model of pneumococcal pneumonia, ARDS, and nonpulmonary organ dysfunction in mice. *American journal of physiology Lung cellular and molecular physiology* 2019: 317(5): L717-L736.

3. Steffen L, Ruppert C, Hoymann HG, Funke M, Ebener S, Kloth C, Muhlfeld C, Ochs M, Knudsen L, Lopez-Rodriguez E. Surfactant replacement therapy reduces acute lung injury and collapse induration-related lung remodeling in the bleomycin model. *American journal of physiology Lung cellular and molecular physiology* 2017: 313(2): L313-L327.

4. Zhu C, Xia L, Li F, Zhou L, Weng Q, Li Z, Wu Y, Mao Y, Zhang C, Wu Y, Li M, Ying S, Chen Z, Shen H, Li W. mTOR complexes differentially orchestrates eosinophil development in allergy. *Scientific reports* 2018: 8(1): 6883.

5. Shen HH, Ochkur SI, McGarry MP, Crosby JR, Hines EM, Borchers MT, Wang H, Biechelle TL, O'Neill KR, Ansay TL, Colbert DC, Cormier SA, Justice JP, Lee NA, Lee JJ. A causative relationship exists between eosinophils and the development of allergic pulmonary pathologies in the mouse. *Journal of immunology* 2003: 170(6): 3296-3305.

6. Konter JM, Parker JL, Baez E, Li SZ, Ranscht B, Denzel M, Little FF, Nakamura K, Ouchi N, Fine A, Walsh K, Summer RS. Adiponectin attenuates lipopolysaccharide-induced acute lung injury through suppression of endothelial cell activation. *Journal of immunology* 2012: 188(2): 854-863.

7. Jacobsen EA, Ochkur SI, Pero RS, Taranova AG, Protheroe CA, Colbert DC, Lee NA, Lee JJ. Allergic pulmonary inflammation in mice is dependent on eosinophil-induced recruitment of effector T cells. *The Journal of experimental medicine* 2008: 205(3): 699-710.

8. Xia LX, Hua W, Jin Y, Tian BP, Qiu ZW, Zhang C, Che LQ, Zhou HB, Wu YF, Huang HQ, Lan F, Ke YH, Lee JJ, Li W, Ying SM, Chen ZH, Shen HH. Eosinophil differentiation in the bone marrow is promoted by protein tyrosine phosphatase SHP2. *Cell death & disease* 2016: 7: e2175.

9. Ochs M, Muhlfeld C. Quantitative microscopy of the lung: a problem-based

approach. Part 1: basic principles of lung stereology. *American journal of physiology Lung cellular and molecular physiology* 2013: 305(1): L15-22.

10. Schneider JP, Ochs M. Stereology of the lung. *Methods in cell biology* 2013: 113: 257-294.

11. Meyerholz DK, Griffin MA, Castilow EM, Varga SM. Comparison of histochemical methods for murine eosinophil detection in an RSV vaccine-enhanced inflammation model. *Toxicologic pathology* 2009: 37(2): 249-255.

12. Levy BD, Kohli P, Gotlinger K, Haworth O, Hong S, Kazani S, Israel E, Haley KJ, Serhan CN. Protectin D1 is generated in asthma and dampens airway inflammation and hyperresponsiveness. *Journal of immunology* 2007: 178(1): 496-502.

13. Oishi Y, Spann NJ, Link VM, Muse ED, Strid T, Edillor C, Kolar MJ, Matsuzaka T, Hayakawa S, Tao J, Kaikkonen MU, Carlin AF, Lam MT, Manabe I, Shimano H, Saghatelian A, Glass CK. SREBP1 Contributes to Resolution of Pro-inflammatory TLR4 Signaling by Reprogramming Fatty Acid Metabolism. *Cell metabolism* 2017: 25(2): 412-427.

14. Miyata J, Fukunaga K, Iwamoto R, Isobe Y, Niimi K, Takamiya R, Takihara T, Tomomatsu K, Suzuki Y, Oguma T, Sayama K, Arai H, Betsuyaku T, Arita M, Asano K. Dysregulated synthesis of protectin D1 in eosinophils from patients with severe asthma. *The Journal of allergy and clinical immunology* 2013: 131(2): 353-360 e351-352.

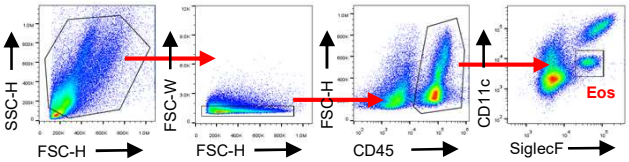


Fig.S1 Simplified gating strategy of pulmonary eosinophils.

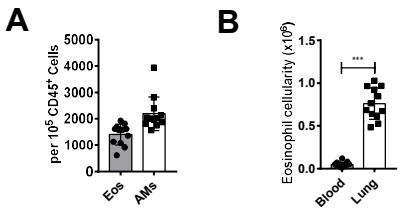


Fig.S2 Amount of pulmonary eosinophils in homeostasis.

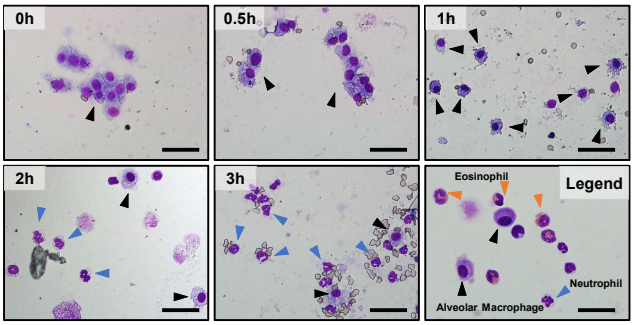


Fig.S3 Morphology of BALF leukocytes after LPS injection.

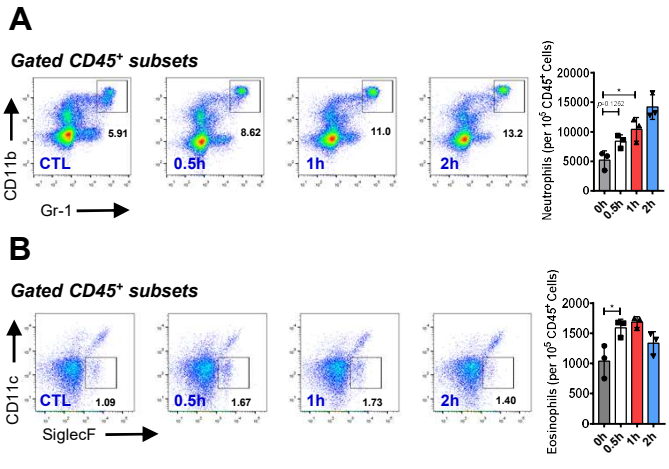


Fig.S4 Early recruitment of pulmonary eosinophils by *S. aureus*.

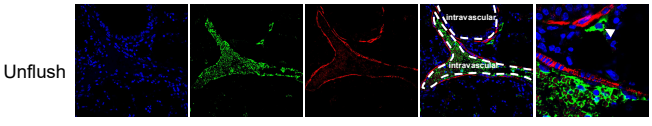


Fig.S5 Distribution of transferred eosinophils.

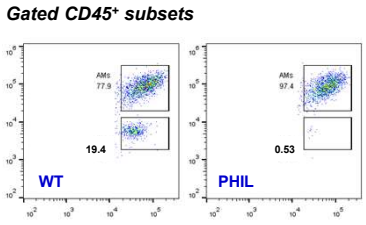


Fig.S6 Depletion of pulmonary eosinophils in PHIL mice.

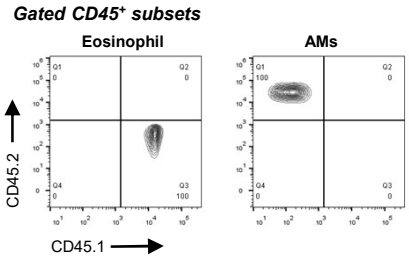


Fig.S7 Repopulation of AMs in chimera mice.

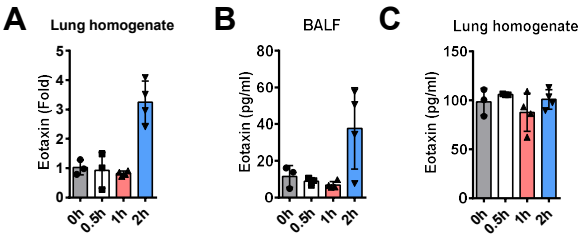


Fig.S8 Expression of eotaxin in lungs post LPS administration.

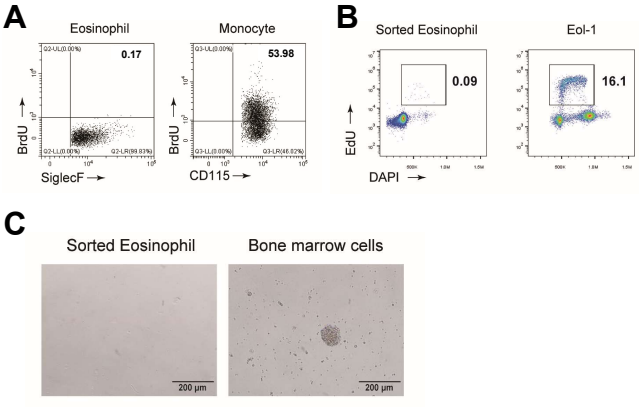


Fig.S9 Proliferative ability of local eosinophils.

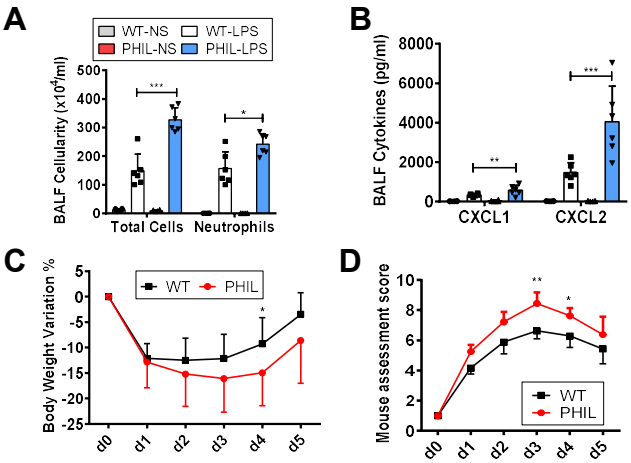


Fig.S10 Pulmonary inflammation and individual status 24h after LPS injection.

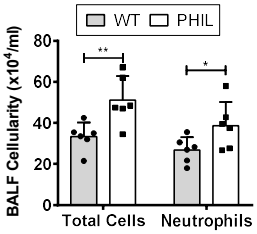


Fig.S11 Exacerbation of pulmonary inflammation in PHIL mice after *S. aureus* infection.

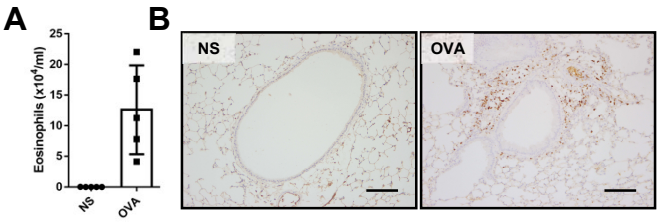


Fig.S12 Eosinophil infiltration in OVA-induced allergic airway inflammation.

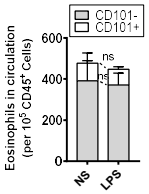


Fig.S13 Eosinophil CD101 expression after eosinophil development related cytokines and allergic pathogen exposure.

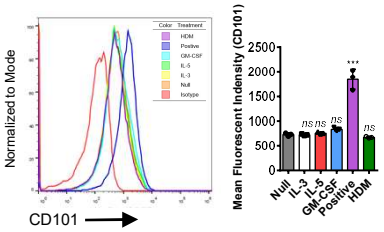


Fig.S14 Eosinophil CD101 expression after eosinophil development related cytokines and allergic pathogen exposure.

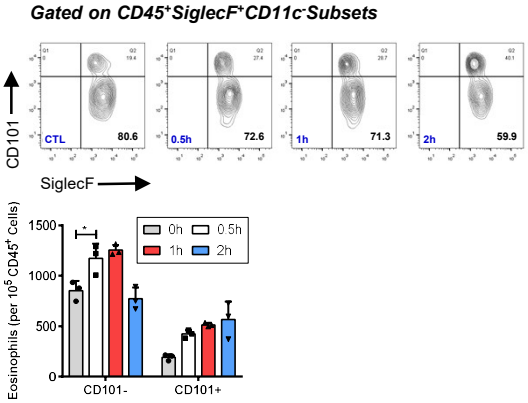


Fig.S15 Subtypes of early-induced eosinophils in *S. aureus* model..

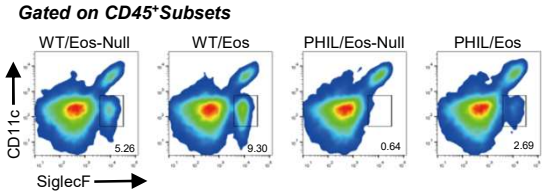


Fig.S16 Efficacy of eosinophil adoptive transfer.

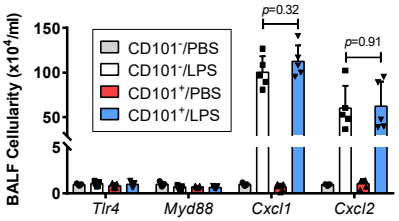


Fig.S17 Inflammatory response of eosinophil subsets post LPS treatment.

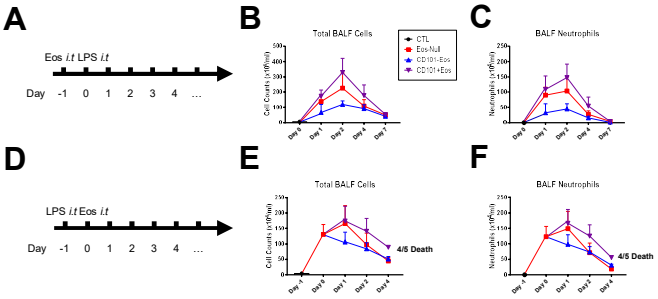


Fig.S18 Prevention and resolution models in eosinophil deficiency mice.